HHS Public Access

Author manuscript

*Neuron*. Author manuscript; available in PMC 2021 September 23.

Published in final edited form as:

*Neuron*. 2020 September 23; 107(6): 1180–1196.e8. doi:10.1016/j.neuron.2020.06.036.

# Developmental attenuation of neuronal apoptosis by neural specific splicing of *Bak1* microexon

**Lin Lin**[1], **Min Zhang**[1], **Peter Stoilov**[2], **Liang Chen**[3], **Sika Zheng**[1,*]

[1]Division of Biomedical Sciences, School of Medicine, University of California, Riverside, CA 92521, USA.

[2]Department of Biochemistry and Cancer Institute, Robert C. Byrd Health Sciences Center, West Virginia University, Morgantown, West Virginia 26506, USA.

[3]Department of Biological Sciences, Quantitative and Computational Biology, University of Southern California, Los Angeles, CA 90089, USA.

## SUMMARY

Continuous neuronal survival is vital for mammals because mammalian brains have limited regeneration capability. After neurogenesis, suppression of apoptosis is needed to ensure a neuron's long term survival. Here, we describe a robust genetic program that intrinsically attenuates apoptosis competence in neurons. Developmental downregulation of the splicing regulator PTBP1 in immature neurons allows neural-specific splicing of the evolutionarily-conserved *Bak1* microexon 5. Exon 5 inclusion triggers nonsense-mediated mRNA decay (NMD) and unproductive translation of *Bak1* transcripts (N-Bak mRNA), leading to suppression of pro-apoptotic BAK1 proteins and allowing neurons to reduce apoptosis. Germline heterozygous ablation of exon 5 increases BAK1 proteins exclusively in the brain, inflates neuronal apoptosis, and leads to early postnatal mortality. Therefore, neural-specific exon 5 splicing and depletion of BAK1 proteins uniquely repress neuronal apoptosis. While apoptosis is important for development, attenuation of apoptosis competence through neural-specific splicing of *Bak1* microexon is essential for neuronal and animal survival.

## eTOC

Lin et al. discover neural-specific splicing of *Bak1* microexon is developmentally programmed to cause neuronal knockout of BAK1 proteins and to reduce neuronal apoptosis. These findings demonstrate that apoptosis attenuation mediated by *Bak1* microexon alone is essential to continuous neuronal and animal survival during development.

*To whom correspondence should be addressed. Lead Contact: Sika Zheng, sikaz@ucr.edu.

AUTHOR CONTRIBUTIONS

L.L. and M.Z. performed bench experiments and analysis, P. S. facilitated the generation of *Bak1* exon 5 knockout founders, L. C. performed the computational biology analysis, S.Z. conceptualized, designed, and administered the project, and wrote the manuscript.

DECLARATION OF INTERESTS

The authors declare no competing interests.

## Graphical Abstract

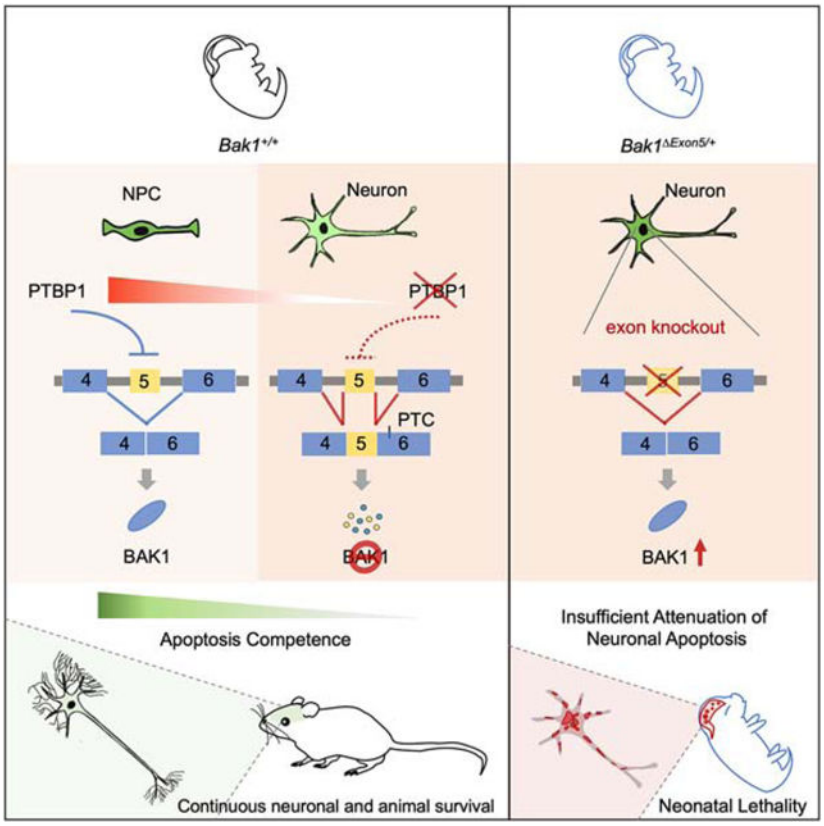


### Keywords

Cell death; PTB; PTBP; PTBP2; BAK; BCL2 family proteins; UPF2; NMD; AS-NMD; Neuronal lifespan; Neural development; Neurogenesis; Alternative splicing

## INTRODUCTION

Apoptosis is a ubiquitous regulated cell death pathway controlling cell turnover and tissue homeostasis in metazoans. Most cells and tissues readily engage apoptosis in response to intrinsic and extrinsic stress. This cellular suicidal program needs to be reined in for mammalian post-mitotic neurons after embryonic neurogenesis is completed. Brain functions cannot be properly formulated without sufficient neurons to establish neural circuits. Similarly, brain functions cannot be maintained when apoptotic neurons break off from existing neuronal connections. The *activation* of neuronal apoptosis has been extensively studied in diseases and after lethal insults, but genetic regulation enforcing *restriction* of neuronal apoptosis is largely unknown.

The multi-BH domain-containing pro-apoptotic proteins BAK1 and BAX of the BCL-2 family is a major decision checkpoint to enter apoptosis (Chipuk et al., 2010; Czabotar et al., 2014; Hardwick and Soane, 2013; Singh et al., 2019; Youle and Strasser, 2008). Apoptosis-inducing developmental cues and cytotoxic stressors act through molecular sensors and

signaling cascades that converge to influence BAX and BAK1's activity on mitochondria. Upon activation, homo- and hetero-oligomerization of BAX/BAK1 forms the mitochondrial outer membrane pore (Hardwick and Soane, 2013; Wang and Youle, 2009), which triggers a sequence of events leading to activation of executioner caspases (CASP3 and CASP7) and subsequent cell destruction.

The action of neurotrophin family is one of the best-known examples of inhibiting neuronal apoptosis (Dekkers and Barde, 2013; Oppenheim, 1989). Pioneering works by Rita Levi-Montalcini and Viktor Hamburger and subsequently many others have established that developing sympathetic neurons critically depend on nerve growth factor (NGF) for survival (Hamburger and Levi-Montalcini, 1949). NGF deprivation-induced apoptosis provides mechanistic support for the dependence of developing sympathetic neurons on NGF (Huang and Reichardt, 2001). This idea is consolidated by the observation that developing peripheral neurons from *Bax*$^{-/-}$ mice are resistant to NGF withdrawal (Deckwerth et al., 1996).

Interestingly, mature sympathetic neurons are independent of NGF for survival (Davies, 1998). To reconcile the difference between developing and mature sympathetic neurons, studies have shown that NGF deprivation in mature neurons up-regulates anti-apoptotic genes including IAPs, miR29b, and miR24 (Benn and Woolf, 2004; Kole et al., 2011, 2013). IAPs binds to and directly inhibits caspase 3, 7, and 9. MicroRNAs miR29 and miR24 target transcripts encoding proapoptotic BH3-only family proteins (Annis et al., 2016). The molecular mechanisms inducing these protective genes are unclear. Other unknowns include the genetic controls by which these anti-apoptotic mechanisms are specific to mature neurons, and why immature neurons are not equipped with the same mechanisms. These observations nevertheless provide early evidence that mature neurons can be restrained from activating apoptosis by engaging multiple redundant anti-apoptotic pathways including transcriptional and miRNA controls.

Alternative pre-mRNA splicing produces multiple mRNA isoforms from a single gene locus and is an essential regulatory mechanism of gene expression in higher eukaryotes. Mammalian brains exhibit prevalent alternative splicing controls (Barbosa-Morais et al., 2012; Merkin et al., 2012). Neural development (e.g., axonogenesis and synaptogenesis) and neuronal activity require various RNA-binding proteins to shape the transcriptome through alternative splicing regulation (Furlanis and Scheiffele, 2018; Raj and Blencowe, 2015; Vuong et al., 2016a; Zheng, 2020). However, the physiological functions of individual alternative splicing events remain mostly unknown. Alternative splicing of apoptosis genes has been documented piecemeal and postulated to encode antagonistic isoforms, mostly supported by ectopic expression of *Fas*, *Casp9*, and *Bcl2l1* cDNA isoforms in cell lines (Paronetto et al., 2016; Schwerk and Schulze-Osthoff, 2005). Physiological relevance of regulating apoptosis genes via alternative splicing has not been shown in animals.

Nonsense-mediated mRNA decay (NMD) is a surveillance mechanism that selectively degrades a transcript containing a premature termination codon (PTC), preventing generation of C-terminal truncated proteins. One widely-recognized NMD-inducing feature is a premature termination codon >50-nucleotide upstream from an exon-exon junction (Chang et al., 2007; Lykke-Andersen and Jensen, 2015; Popp and Maquat, 2013;

Rebbapragada and Lykke-Andersen, 2009). Regular transcripts are immune to NMD because normal termination codons are usually in last exons.

Alternative splicing coupled to NMD (AS-NMD) can post-transcriptionally influence gene outputs. Specifically, alternative splicing can produce an NMD sensitive isoform when an alternative exon contains an in-frame (early) stop codon or its inclusion shifts the reading frame to generate a downstream PTC (Giorgi et al., 2007; McGlincy and Smith, 2008; Zheng, 2016; Zheng and Black, 2013). AS-NMD is best known to maintain homeostatic expression of some splicing factors via self-regulatory negative feedback loops and has been implicated in fine-tuning expression of other genes (Boutz et al., 2007; Lareau et al., 2007; Ni et al., 2007; Rossbach et al., 2009; Spellman et al., 2007; Valacca et al., 2010; Yan et al., 2015). However, the genetic necessity for AS-NMD regulation and the functional significance of any NMD-associated alternative splicing events have not been demonstrated in the context of a whole organism.

In this study, we systematically examined alternative splicing regulation of the apoptosis pathway during brain development. We reasoned that neurons transform their control of apoptosis genes to allow uninterrupted survival. Our systematic searches identified one essential genetic regulatory module for neurons to fend off apoptosis: developmental depletion of pro-apoptotic protein BAK1 through neural-specific splicing of a *Bak1* microexon. Using combinatorial approaches including CRISPR knockout of the neural-specific *Bak1* microexon in mice, we show apoptosis attenuation through alternative splicing programming is necessary for neuronal and animal survival.

## RESULTS

### Unbiased identification of *Bak1* exon 5 associated with neural-specific regulation of apoptosis

If alternative splicing is important for uniquely repressing apoptosis in neurons, some apoptosis-regulatory genes would undergo differential splicing between neural and non-neural tissues, since many non-neural cells constantly undergo apoptosis induced by intrinsic and extrinsic stress. We investigated neural-specific alternative splicing of 1,821 apoptosis genes (all genes with a term “Apoptosis” in the Gene Ontology Consortium) using adult mouse tissue RNA-seq data generated by ENCODE. We calculated percent spliced in (PSI) of each cassette exon as a measure of alternative splicing levels (Methods). Unbiased hierarchical clustering of tissues and exon PSIs shows most alternative exons of apoptosis genes exhibit similar splicing across tissues (Figure 1A). However, three small exon clusters are associated with neural tissues: the mean of ΔPSI between neural and non-neural tissues was 45.6, −24.3, −68.1, respectively (Figure S1A, Table S1). Interestingly, neural tissues cluster most closely with heart tissues: cardiac muscle cells also need to survive for a long time.

We investigated the temporal pattern of apoptosis sensitivity in developing cortical neurons and found their apoptosis competence is gradually lost during differentiation. Specifically, we cultured primary cortical neural progenitor cells (NPC) and primary cortical neurons from embryonic day 14 mice and treated the cells with 0.5 μM staurosporine (STS, a widely-

used apoptosis inducer) or DMSO control (Figure S2A). Our NPC cultures typically comprise 98% Nestin+ cells before treatment. Nestin+ cells remained in about 97% of the NPC cultures post DMSO treatment, and 88% post STS treatment (Figure S2B). STS probably diminished Nestin levels and some dying cells appeared to lose Nestin staining faster than DAPI staining. To account for this difference, we quantified cell death in NPC cultures as the percentage of cleaved Caspase 3 positive (CC3+) cells among Nestin+ cells (CC3+ Nestin+ /Nestin+) and found 37.8% of Nestin+ cells underwent apoptosis after STS treatment, representing a 13-fold increase in cell death compared to DMSO treatment (Figure S2C).

Our primary neuronal cultures comprise about 97% MAP2+ cells (Figures S2D-G). Because MAP2 and Tau1 staining becomes sinuous and extensive by 5 and 7 days *in vitro* (DIV), we chose NeuN for quantification. The percentage of NeuN+ cells increased from DIV 3 to DIV 7 due to increasing NeuN expression over time. The percentages of NeuN+ cells in the culture were not affected by STS treatment (Figure S2F).

To quantify the sensitivity to apoptosis at each developmental stage, fold changes were derived by normalizing cell death percentages upon STS treatment to those with DMSO treatment. As shown in Figure S2C, the normalized fold change was the highest in NPCs. More importantly, apoptotic cell death after STS treatment gradually decreased such that DIV 7 primary neurons were no longer responsive to STS treatment. Therefore, neurons must transform how they regulate apoptosis during development by yet to-be-identified mechanisms. In this study we focus on alternative splicing regulation.

Since neurons become increasingly resistant to apoptosis during early differentiation, we investigated developmental programming of alternative exons of apoptosis genes using RNA-seq data of mouse forebrains (GSE84803 and GSE149491) from embryonic day 12 (E12), 14, 17, and postnatal day 2 (P2, equivalent to DIV 7 neurons but not exact). Unbiased clustering defined five exon groups, two of which are developmentally regulated (Figures 1B, S1B, Table S2, Methods). We performed similar analysis using the ENCODE midbrain transcriptome data and identified one developmentally-programmed exon cluster (Figure S1C, Table S3).

We compared developmentally-programmed and neural-enriched alternative splicing events to identify the overlap (Figure 1C for forebrain, Figure S1D for midbrain). These genetically programmed exons might uniquely control neuronal apoptosis competence and thereby support neurons' uninterrupted survival. Among them is *Bak1* exon 5, a 20-nt microexon, which appears in both the forebrain and midbrain datasets (Figures 1C, S1D). Other interesting targets include alternative exons in *Bin1, Dpf2*, *Mef2a*, and *Mef2d*, etc.

We performed quantitative capillary electrophoresis to assay splicing and verified the developmental changes of these exons in cortices from E12 to P2 (Figures 1D-G). Most displayed the largest splicing changes between E12 and E16, indicating genetic programming of these exons occurs during early development, long before neurons establish and mature their synaptic connections. It is also consistent with the observation that apoptosis attenuation starts in the earliest stage of differentiation (Figure S2). We decided to

focus on *Bak1* because it is an essential part of the core apoptosis pathway. Strikingly, we found *Bak1* exon 5 inclusion only in neural tissues, suggesting its unique association with regulation of neuronal apoptosis (Figure 1H).

## Exon 5 splicing leads to NMD and unproductive translation of *Bak1* transcripts

Normal BAK1 protein is translated from the exon 5 exclusion ($E5^-$) isoform with a stop codon in exon 7 (Figure 2A). Exon 5 inclusion results in a frame shift and termination of the reading frame at a conserved premature stop codon in exon 6, making the inclusion isoform a possible target of NMD. Previously, Arumae's group detected the exon 5 inclusion isoform ($E5^+$) using RNase protection assay and indicated its neural specific expression (Sun et al., 2001). They proposed this isoform encoded a truncated BH3-only N-Bak protein and further suggested that the mRNA of N-Bak escaped NMD (Jakobson et al., 2012; Sun et al., 2001).

To test whether the exon 5 inclusion isoform is targeted by NMD, we knocked out the essential NMD factor UPF2 in the mouse cortex using Emx1-Cre line and measured the expression of $E5^+$ and $E5^-$ isoforms separately. We found the $E5^+$ isoform was substantially up-regulated by about 6.6-fold at each developmental age (E14.5, E15.5, E17.5 and P1) and the $E5^-$ isoform was marginally changed (Figure 2B). If *Upf2* knockout affected *Bak1* transcription, both $E5^+$ and $E5^-$ isoforms should have been simultaneously up- (or down-) regulated in the same direction. If *Upf2* knockout affected exon 5 splicing, the two isoforms should have changed in opposite directions. Neither scenario agrees with the data (Figure 2B). Therefore, upregulation of $E5^+$ isoform in the *Upf2* conditional knockout was due to NMD inhibition.

To further test whether the upregulation of $E5^+$ isoform in the *Upf2* conditional knockout could be due to transcriptional regulation, we performed RT-qPCR to measure the *Bak1* nascent RNA transcript. Our results showed that the amounts of *Bak1* nascent RNA did not change by *Upf2* knockout (Figure S3A). NMD inhibition by cycloheximide treatment also substantially increased the $E5^+$ isoform (Figure S3B). These data taken together confirm that the $E5^+$ isoform is subject to NMD. Consistent with the notion that NMD targets are translationally repressed (Chang et al., 2007; Popp and Maquat, 2013), we have been unable to detect the presumptive protein encoded by the $E5^+$ isoform.

We found exon 5 splicing is correlated with diminished BAK1 protein. BAK1 proteins were down-regulated in embryonic neocortices (Figure 2C), coinciding with the ending phase of neurogenesis and the period of increasing exon 5 inclusion (Figure 1D). Adult neural tissues express mostly the $E5^+$ isoform but little BAK1 proteins. Note that the alternative splicing assay of *Bak1* exon 5 only showed the relative ratios of the two isoforms and did not reflect isoform expression levels nor their individual temporal changes (Figure 1D). Theoretically, despite a developmental increase in exon 5 inclusion, the absolute $E5^-$ isoform level could still increase instead of decrease. To test whether the *Bak1* translational isoform ($E5^-$) is reduced during development to cause loss of BAK1 protein, we performed isoform-specific RT-qPCR. The $E5^-$ isoform was indeed downregulated during embryonic cortical development whereas the $E5^+$ isoform was upregulated (Figure 2D). The opposite trends of the two isoforms also confirm alternative splicing regulation of exon 5 during this period.

Taken together, BAK1 protein expression originates from the E5$^{-}$ isoform and higher exon 5 inclusion reduces BAK1 protein expression. As NMD targets are translationally unproductive and rapidly degraded, neuronal suppression of the BAK1 protein is due to preferential expression of the *Bak1* NMD isoform. Indeed, as *Bak1* nascent RNA (proxy of *Bak1* transcription) appears to increase during development (Figure S3A), exon 5 splicing coupled to NMD would be the major mechanism of repressing BAK1 protein expression.

## Developmental regulation of *Bak1* splicing is conserved

Human *BAK1* has a 20-nt exon (exon 5) that is almost identical to mouse *Bak1* exon 5. We analyzed the human Genotype-Tissue Expression (GTEx) data for *BAK1* exon 5 splicing. GTEx profiled the expression of 54 non-diseased tissues from nearly 1,000 individuals. We found exon 5 inclusion was overwhelmingly present in neural tissues and largely missing in non-neural tissues (Figure 3A). We also analyzed RNA-Seq data from the Illumina Human Body Map 2.0 project that profiled 16 human tissues (GSE30611). The result consistently showed that *BAK1* exon 5 splicing is uniquely and substantially higher in the brain than any other tissue (Figure S3C).

To examine whether human exon 5 inclusion is established as in mice during differentiation, we analyzed RNA-seq data from *in vitro* differentiation of human and mouse embryonic stem (ES) cells (human data from ENCODE: ENCFF000FCX, ENCFF585VNQ, ENCFF509QEV; mouse data from GSE71179). In both cases, exon 5 is skipped in ES cells and ES cell-derived neural progenitors but is included in differentiated neurons (Figures 3B-C). Exon 5 and its flanking intronic sequences are conserved, possibly containing *cis*-regulatory elements under evolutionary selection for alternative splicing control of exon 5 (Figures 3B-C, Figure S3D). As exon 5 splicing is switched on in postmitotic neurons but not in NPCs, NPCs express more BAK1 proteins than primary cortical neurons (Figures 3D-E).

To test whether *BAK1* exon 5 is developmentally regulated in the human brain, we analyzed the RNA-seq data from the Human Developmental Biology Resource (HDBR) that profiled prenatal human brains (Lindsay et al., 2016). As shown in Figure 3F, the PSI values of human BAK1 exon 5 in developing brains gradually increased from 25 at 8 weeks post conception to around 80 at 14–17 weeks post conception.

We found the premature termination codon (PTC: UGA) in exon 6 of the E5$^{+}$ isoform is conserved among all annotated mammals (and lizard), indicating selection pressure on AS-NMD regulation of *Bak1* (Figure 3G). Notably, the E5$^{-}$ isoform codons (NUG, ANN) overlapping the E5$^{+}$ PTC have both synonymous and non-synonymous variants outside of UGA, suggesting that the selection pressure is specifically imposed on the PTC rather than the BAK1 (E5$^{-}$ isoform) coding sequence. Furthermore, if not for evolutionary constraints to retain this PTC in the E5$^{+}$ isoform, the [(C/U)UG] codon in the E5$^{-}$ isoform could have synonymous variants [(C/U)UN].

The lack of BAK1 protein expression in neural tissues is conserved between human and mouse. Mass spectrometry analysis from the Human Proteome Map project revealed the absence of BAK1 protein in all analyzed neural tissues (frontal cortex, spinal cord, and

retina, Figure 3H). BAK1 protein was not detected in the human liver or pancreas by the Human Proteome Map project using mass spectrometry but was detected in the mouse liver by Western blots (see below).

## Heterozygous deletion of *Bak1* exon 5 dis-inhibits BAK1 protein expression in the mouse brain

If AS-NMD regulation represses BAK1 and reduces apoptosis competence in neurons, then abolishing the regulation *in cis* will up-regulate the BAK1 protein and alter neuronal susceptibility to apoptosis. To test this, we designed and screened sequence-specific guide RNAs in the flanking intronic sequences to delete exon 5 using CRISPR/Cas9. We then used CRISPR to knock out exon 5 in mice so that the edited allele constitutively spliced from exon 4 to exon 6 and generated only the $E5^-$ isoform (Figure 4A), abrogating the transition from $E5^-$ to $E5^+$ isoforms during brain development. ES cells, NPCs, and non-neural tissues do not include exon 5. Therefore, they should not be affected by exon 5 deletion. We generated genetically-mosaic founders in the C57BL/6 background, which were subsequently crossed with wildtype (*WT*) mice to obtain germline-transmitted heterozygotes ($Bak1^{\Delta exon5/+}$). Targeted exon deletion in mice was verified by PCR genotyping (Figure 4B) and Sanger sequencing.

We tested the splicing of exon 5 in $Bak1^{\Delta exon5/+}$ and *WT* control littermates. At birth, $Bak1^{\Delta exon5/+}$ mice showed a decrease in the $E5^+$ isoform and an increase in the $E5^-$ isoform in various brain regions, further confirming the exon knockout (Figure 4C). Importantly, the inclusion ratio in the heterozygous cortex was consistent with the following mathematical prediction considering the NMD effect. We determined the NMD efficiency of *Bak1* $E5^+$ isoform as the ratio of *Bak1* $E5^+$ isoform in Upf2cKO cortices relative to *Bak1* $E5^+$ isoform in control littermates, or 6.6-fold (Figure 2B). This estimation of NMD efficiency was independently validated by CHX treatment, which shows a 6.4-fold upregulation of *Bak1* $E5^+$ isoform upon NMD inhibition (Figure S3B). In P0 WT cortices, 71% of total steady-state *Bak1* transcripts were $E5^+$ NMD transcripts (Figure 1G). In $Bak1^{\Delta exon5/+}$ cortices, half of the transcribed *Bak1* transcripts were no longer spliced to be the $E5^+$ NMD isoform but spliced to be the $E5^-$ isoform. Therefore, the expected inclusion ratio of *Bak1* exon 5 in $Bak1^{\Delta exon5/+}$ cortices is

$$\frac{E5^+\text{isoform}}{E5^+\text{isoform} + E5^-\text{isoform}} \text{ or } \frac{71 \div 2}{71 + 2 + (29 + 71 + 2 \times 6.6)} = 11.9\%$$

This mathematically-predicted ratio (11.9%) is similar to the mean of experimental measurements (11.2%, Figure 4C).

As expected, decreased exon 5 inclusion up-regulated the BAK1 protein (Figures 4D-E). These were seen in all brain regions (Figures 4C-E), demonstrating the ubiquitous AS-NMD regulation of *Bak1* throughout the brain. Up-regulation of the BAK1 protein is correlated with the increase in the $E5^-$ isoform. Isoform-specific RT-qPCR showed that the $E5^-$ isoform increased by about 10-fold and the $E5^+$ isoform was significantly down-regulated in P0 cortices (Figure 4F). These measurements are consistent with the mathematical

prediction incorporating the NMD effect, as the fold change for the E5$^{-}$ isoform in the *Bak1*$^{\Delta exon5/+}$ P0 cortex is predicted to be about 9-fold (i.e., $\frac{29+71\div 2\times 6.6}{29}=9.08$ ).

## The phenotypes of *Bak1*$^{\Delta exon5/+}$ mice

To test whether up-regulation of BAK1 protein sensitizes neurons to apoptosis, we stained *Bak1*$^{\Delta exon5/+}$ and *WT* littermate brains with the cleaved Caspase3 (CC3) antibody and quantified apoptotic cells. The *Bak1*$^{\Delta exon5/+}$ brain displayed more CC3 signals than the WT brain. At P2, apoptotic cells increased by 2-fold in the mutant hippocampus (Figures 5A-B, 68.0 in the hemi-hippocampus of *Bak1*$^{\Delta exon5/+}$ per brain slice vs 34.5 in the WT). The mutant cortex exhibited a 2.7-fold increase in apoptotic cells (Figures S4A-B). CC3+ cell numbers further increased at P3, indicating that the phenotype worsened over time. For example, the mutant hippocampus showed a 3.1-fold increase in CC3+ cells (Figures 5A, 5C, 122.8 in the hemi-hippocampus of *Bak1*$^{\Delta exon5/+}$ per brain slice vs 39.2 in the WT). Notably, *Bak1*$^{\Delta exon5/+}$ mice exhibited a lower brain weight, consistent with the increased cell death (Figures S4C-D).

We tested whether exon 5 deletion affected neural progenitor cells. As shown in Figures S5A-D, about 79% of cells in the WT E12 cortex were PAX6+ neural stem and progenitor cells, and this percentage was unaffected in *Bak1*$^{\Delta exon5/+}$ cortices. Furthermore, neither the percentage of (CC3+ PAX6+) apoptotic cells among neural progenitor cells nor the percentage of total (CC3+) apoptotic cells changed in the *Bak1*$^{\Delta exon5/+}$ cortex compared to the WT. Therefore, increased apoptotic susceptibility is only limited to differentiated neurons.

Next, we examined what neuronal subtypes undergo cell death. We focused on the hippocampus over other brain regions because of its well-defined structure and boundary. We stained P3 WT and *Bak1*$^{\Delta exon5/+}$ brains with antibodies against cleaved Caspase 3 (CC3) and glutamatergic neuronal marker NEUROD2. As shown in Figure S5E, NEUROD2 stained CA1 and CA3 pyramidal neurons. On average, we counted 17.0 CC3+ NEUROD2+ cells in the WT hemi-hippocampus per brain slice, representing about 43% of total CC3+ cells in the region. In the *Bak1*$^{\Delta exon5/+}$ hemi-hippocampus, we counted 33.1 CC3+ NEUROD2+ cells per brain slice, showing that exon 5 deletion augmented apoptotic cell death of pyramidal neurons in the hippocampus by about 2-fold (Figures S5E-G).

Subtracting CC3+ NEUROD2+ cells from total CC3+ cells, there were 22.2 CC3+ NEUROD2− cells in the WT and 89.7 in the *Bak1*$^{\Delta exon5/+}$ mutant (or a 4-fold increase). Therefore, NEUROD2− cells are more sensitive to apoptosis upon exon 5 deletion than NEUROD2+ cells. We note that NEUROD2 labels most, if not all, pyramidal neurons in the hippocampus, and the dentate granule cell layer rarely stain positive for CC3+ at P2 and P3 (Figures 5A, S5E). Assuming exon 5 deletion affects neurons but not neural progenitors or glia in P3 hippocampus, the *surplus* CC3+ NEUROD2− cells in *Bak1*$^{\Delta exon5/+}$ are likely apoptotic inhibitory neurons. We tested GABAergic neurons using GAD67 antibodies. Unfortunately, GAD67 staining was diffuse and sometimes without clear cellular boundaries in the P3 hippocampus, obstructing accurate quantification. This analysis shows that different groups of neurons (NEUROD+ vs NEUROD−) can have different vulnerabilities to

apoptosis and suggests inhibitory neurons are possibly more affected by exon 5 deletion than excitatory pyramidal neurons in the P3 hippocampus.

To further confirm the phenotype was due to increased susceptibility to apoptosis, we sensitized mutant and WT primary cortical neurons with staurosporine (STS). First, we verified that exon 5 inclusion was reduced and the BAK1 protein was induced in the *Bak1*$^{\Delta exon5/+}$ primary neurons (Figures 5D-E). NPCs displayed no change in either exon 5 splicing or BAK1 protein expression, consistent with the notion that exon 5 knockout does not affect NPC. We note that the percentage of Nestin+ cells in primary NPC cultures and the percentage of NeuN+ cells in primary neuronal cultures remain unaffected by heterozygous deletion of exon 5 (Figures S6A-D). After STS treatment, mutant neurons exhibited enhanced cell death, which was normalized by Caspase inhibitors (Figure 5F). Therefore, post-mitotic *Bak1*$^{\Delta exon5/+}$ neurons retain a higher sensitivity to apoptosis.

*Bak1*$^{\Delta exon5/+}$ mice die within 4 days after birth (Figure 5G). We noticed the absence of a milk spot in *Bak1*$^{\Delta exon5/+}$ mice (Figure S4E), suggesting mutant mice could die from failure in feeding. Supporting this notion was a lack of weight gain in *Bak1*$^{\Delta exon5/+}$ mice after birth (Figures 5H-I). Non-neural tissues showed no change in *Bak1* exon 5 splicing or BAK1 protein expression (Figures S7A-C). Additionally, we detected no obvious abnormalities in non-neural tissues (Figure S7D), indicating that the phenotype was specific to and originated from the nervous system. Given the ubiquitous AS-NMD regulation of *Bak1* expression in the nervous system, it is conceivable that in *Bak1*$^{\Delta exon5/+}$ mice certain essential neural circuits for organism survival fail to function due to increased cell death.

## PTBP1 inhibits *Bak1* exon 5 splicing and modulates apoptotic sensitivity

We examined how exon 5 splicing is developmentally programmed and found *Bak1* exon 5 is inhibited by polypyrimidine-tract binding protein PTBP1. PTBP1 is an RNA binding protein that regulates alternative exon splicing often through interactions with flanking introns (Kafasla et al., 2012; Keppetipola et al., 2012). Using the ENCODE eCLIP datasets, we found that PTBP1 protein interacts with *BAK1* pre-mRNA transcripts in both K562 and HepG2 cells (Figure 6A). Importantly, PTBP1 specifically and most strongly binds the conserved intronic sequence proximal to the 3' splice site of exon 5.

To test whether PTBP1 regulates exon 5 splicing, we performed gain and loss of function studies in N2a cells. PTBP1-overexpression repressed *Bak1* exon 5 splicing and consequently up-regulated the BAK1 protein (Figures 6B and S8A-E). Conversely, depletion of PTBP1 with either of two independent siRNAs increased *Bak1* exon 5 splicing and reduced the BAK1 protein (Figures 6C-F). Interestingly, *Bak1* exon 5 splicing is insensitive to PTBP2, the PTBP1 paralog predominantly expressed in post-mitotic neurons (Markovtsov et al., 2000; Polydorides et al., 2000; Zhang et al., 2019). PTBP2 induction upon PTBP1 depletion was not correlated with exon 5 skipping. Reducing PTBP2 in conjunction with PTBP1 knockdown did not affect exon 5 splicing more than single PTBP1 knockdown (Figures S8F-H). Therefore, exon 5 splicing may be additionally regulated by PTBP1-specific cofactors.

Since PTBP1 controls BAK1 abundance, we hypothesized that PTBP1 could modulate cell sensitivity to apoptosis. Using FACS with annexin V and propidium iodide (PI) staining, we found PTBP1 depletion significantly decreased early apoptotic cell proportions (annexin V+, PI-) after induction of apoptosis with staurosporine (Figures 6G-H). Cleaved Caspase 3 was also significantly lower in PTBP1-depleted cells (Figures 6D, 6I).

To further confirm whether PTBP1 directly regulates *Bak1* exon 5 splicing, we searched the flanking introns and identified a stretch of CU-alternating sequence reminiscent of PTBP1 binding sites. This sequence is conserved between human and mouse (with one nucleotide difference) and is bound by PTBP1 (Figure 6A). We generated a chimeric minigene by inserting *Bak1* exon 5 and its flanking intronic sequences into a backbone minigene reporter (Figure 6J). PTBP1 knockdown increased exon 5 splicing in the minigene reporter from 2% to 24% (Figure 6K). We mutated the PTBP1 binding site to disrupt alternation of C and U. Agreeing with loss of PTBP1 inhibition, the baseline exon 5 inclusion in the mutant minigene increased, and the mutant minigene splicing was no longer responsive to PTBP1 knockdown (Figure 6K). Taken together, we concluded PTBP1 directly inhibits *Bak1* exon 5 splicing.

### Developmental PTBP1 loss is necessary for inhibiting BAK1 proteins in the mouse brain

As PTBP1 protein is downregulated during embryonic brain development (Figure 7A), we propose the PTBP1 loss upregulates *Bak1* exon 5 splicing and downregulates BAK1 proteins, resulting in a decrease of neurons' intrinsic sensitivity to apoptosis. In support of this, *Bak1* splicing and protein expression closely mirror the temporal expression of PTBP1 in cortices (Figures 1D, 7A). Furthermore, the BAK1 and PTBP1 proteins are spatially correlated in developing cortices at various embryonic ages (Figures 7B-G).

To further test whether PTBP1 loss is necessary for BAK1 downregulation *in vivo*, we delivered a PTBP1-expressing plasmid (CAG-FLAG-PTBP1-IRES-EGFP) to neural progenitor cells in the neocortex by *in utero* electroporation (IUE) at E14.5 to counteract developmental PTBP1 loss (Figure 7H). At E18.5 PTBP1-expressing $GFP^+$ neurons migrated outside the PAX6+ ventricular zone and were PAX6 negative (Figure S9A). Many of them already stained positive for upper layer neuronal marker Satb2 (Figure S9B). Furthermore, PTBP1-expressing $GFP^+$ post-mitotic neurons showed reduced expression of PTBP2, confirming the functional activity of the ectopic PTBP1 (Figure S9C). Many PTBP1-expressing $GFP^+$ post-mitotic neurons exhibited abnormally high BAK1 protein expression above the background, and the BAK1 protein level was positively correlated with the ectopic PTBP1 level (Figures 7I-R). Additionally, cleaved Caspase3 staining is increased in the IUE hemisphere compared to the contralateral hemisphere (Figures S10A-B). These data show PTBP1 positively controls BAK1 protein expression in a dose-dependent manner *in vivo* and PTBP1 loss mediates the reduction of the BAK1 protein and neuronal apoptosis.

## DISCUSSION

In this study, we show selective repression of pro-apoptotic BAK1 protein and attenuation of apoptosis competence in neurons are intrinsically programmed during embryonic brain development and are absolutely required for animal survival. Suppression of the BAK1

protein is ensured by a robust genetic regulatory module encompassing activation of exon 5 splicing and NMD and unproductive translation of the $E5^{+}$ isoform (Figure 7S). Neuronal differentiation sets this intrinsic programming in motion by down-regulating exon 5 repressor PTBP1. As a result, exon 5 is spliced exclusively in neural tissues leading to neural-specific "knockout" of BAK1. This regulation is unlikely the sole mechanism supporting continuous neuronal survival but is so essential that heterozygous deletion of its central element (*Bak1* exon 5) is enough to increase neuronal apoptosis and cause animal lethality.

Comparison between $Bak1^{\Delta exon5/+}$ and $Bak1^{-/-}$ mice is interesting. $Bak1^{-/-}$ mice with homozygous deletion of exons 2–6 are viable, fertile, and have no detectable phenotypic abnormalities (Lindsten et al., 2000). In contrast, $Bak1^{\Delta exon5/+}$ mice (with the deletion of exon 5 in a single allele) cannot survive. The severer phenotype in $Bak1^{\Delta exon5/+}$ mice is not due to the size of deletion but demonstrates the intricate regulation of genetic elements through the control of RNA processing. As exon 5 does not encode the regular BAK1 protein, it showcases essential roles of regulatory elements outside of protein coding sequences. The phenotypic contrast originates from the opposite impacts of their genetic deletions on BAK1 protein expression. $Bak1^{-/-}$ eliminates BAK1 protein but has no phenotypes because of the negligible BAK1 expression in the brain and BAX compensation in peripheral tissues. $Bak1^{\Delta exon5/+}$ does not affect peripheral tissues but substantially increases BAK1 protein expression in the brain. The latter leads to increased neuronal apoptosis and early mortality. It will be interesting to dissect the neural circuits impaired in $Bak1^{\Delta exon5/+}$ that are essential for neonatal survival. Because $Bak1^{\Delta exon5/+}$ mice cannot be propagated, we are generating a conditional allele for future analysis. Taken together, mice can tolerate whole-body BAK1 loss but not neural-specific BAK1 gain. Moreover, a small percentage of triple knockout mice of *Bak1* and its close paralogs *Bax* and *Bok* appeared largely normal, suggesting mouse development or survival do not absolutely require activation of apoptosis (Ke et al., 2018). The phenotypes of $Bak1^{\Delta exon5/+}$ mice, on the other hand, show that apoptosis suppression in neurons is necessary for mouse survival.

Exon 5 is included only in neural tissues. Using RNA-seq data and quantitative splicing assays, our unbiased screen and systematic approaches (comparing 54 human tissues of nearly a thousand individuals in GTEx, 16 human tissues from Illumina Human Bodymap 2.0, 16 mouse tissues from ENCODE, 10 stages of human developing brains, 6 stages of mouse developing forebrains, and 8 stages of mouse developing midbrain) firmly established the neural-specific splicing and the temporal induction of exon 5. As far as we know, no other genes have been demonstrated to adopt AS-NMD control to the extreme as *Bak1* does, where exon splicing induces natural "knockout" of the protein product in certain tissues. Neither have there been reports to showcase the physiological relevance of an AS-NMD control through genetic ablation of an NMD-associated exon. Although additional mechanisms might regulate *Bak1* expression, AS-NMD control of *Bak1* alone has a life-or-death impact on neuronal and animal survival. Our findings therefore solidify the functional significance of AS-NMD as an essential regulatory mechanism (Zheng, 2016)

A major repressor of exon 5 splicing is PTBP1, which is almost ubiquitously expressed in peripheral tissues but missing in the adult brain (Kafasla et al., 2012; Keppetipola et al.,

2012). Therefore, PTBP1 contributes to inhibiting exon 5 outside of the brain. In the developing brain, PTBP1 is reduced, allowing exon 5 inclusion. It is interesting that PTBP2 is not a potent inhibitor as PTBP1. Possible explanations include PTBP1-specfiic co-factors and PTBP2-specific antagonizing factors that coordinately influence exon 5 splicing. These regulators, and other RNA binding proteins that directly control exon 5 splicing, still need to be identified.

The exon 5 inclusion isoform was proposed to encode a truncated BH3-only N-Bak protein and escape NMD (Jakobson et al., 2012; Sun et al., 2001). The conclusion is based on the observation that concurrent treatment of cycloheximide (which blocks NMD) and actinomycin D (which inhibits polymerase II-mediated transcription) marginally increased N-Bak mRNA compared to DMSO treatment. However, transcription inhibition and NMD inhibition counteract each other in affecting steady-state mRNA levels. Given that transcription inhibition of *Bak1* should have reduced its steady-state mRNA levels, the N-Bak mRNA ($E5^+$ isoform) was up-regulated by cycloheximide (as we have shown in Figure S3B).

We provided multiple lines of genetic and biochemical data that firmly established $E5^+$ isoform as an NMD substrate. First, genetic ablation of NMD up-regulates the $E5^+$ isoform (Figure 2B). Second, pharmacological inhibition of NMD up-regulates the $E5^+$ isoform (Figure S3B). Third, independent mass spec analysis has not detected any BAK1 peptides in the brain (Figure 3H), agreeing with loss of BAK1 protein due to NMD and unproductive translation of the $E5^+$ isoform. Note that the hypothetical BH3-only N-Bak protein has not been shown in the literature either.

Fourth, *Bak1* splicing and isoform expression in the $Bak1^{\Delta exon5/+}$ brain are only consistent with the $E5^+$ isoform being selectively targeted by NMD. All pre-mRNA transcripts from the $Bak1^{\Delta exon5}$ allele are spliced to produce the $E5^-$ isoform. If the $E5^+$ isoform was not subject to NMD but underwent similar decay as the $E5^-$ isoform, exon 5 inclusion in the $Bak1^{\Delta exon5/+}$ P0 cortex would be 35.5% (half of 71% based on Figure 1G), and the $E5^-$ isoform would be up-regulated by 2.2-fold: ($\frac{29+71\div2}{29}=2.22$). Neither of these predictions were correct: in the $Bak1^{\Delta exon5/+}$ P0 cortex, exon 5 inclusion was 11.2%, and the $E5^-$ isoform was increased by about 10-fold (Figures 4C, 4F), in line with our experimental measurement. The lower-than-expected exon 5 inclusion and the higher-than-expected induction of the $E5^-$ isoform indicate the $E5^+$ isoform was less stable than the $E5^-$ isoform.

We show that developmental repression of BAK1 expression through AS-NMD intrinsically attenuates apoptosis competence in neurons to support continuous neuronal survival (Figure S11A). Our discoveries complement existing models and theories that highlight extrinsic signals and reactive responses to enhance neuronal survival. Two of the best studied extrinsic survival signals are neurotrophins in the peripheral nervous system and synaptic activity in the central nervous system. The “neurotrophic theory” and the “activity-dependent survival theory” assume the default cell fate of neurons is death and emphasize that neuronal survival is directed by target cells/tissues (Figures S11B-C). To survive, neurons need target-derived trophic factors in the peripheral nervous system and/or appropriate synaptic transmission in the central nervous system (Ghosh et al., 1994; Mao et al., 1999; Oppenheim, 1989).

Interestingly, apoptosis sensitivity of cortical neurons progressively decreases during differentiation even before synapse formation (Figure S1). Apoptotic resistance therefore is not a “toggle switch” imposed only by fruitful neuronal connections (or reaching target tissues/cells), as previously suggested. Since a post-mitotic neuron’s lifespan includes the time spent as an immature neuron and even immature neurons need to live weeks (in rodents) and months (in humans) before forming functional neural circuits, programming of apoptosis resistance apparently starts as early as neuron birth.

Another mechanism to maintain survival of peripheral neurons in response to NGF deprivation is to up-regulate anti-apoptotic genes, e.g., miR29b and XIAP (Figure S11D). This “reactive” mechanism has been depicted as “apoptosis brakes” (Annis et al., 2016; Benn and Woolf, 2004). Neurons have multiple redundant brakes to deploy, because knockout mice of each IAP member and compound null mutants exhibit normal development and lack obvious phenotypes (Conze et al., 2005; Harlin et al., 2001; Heard et al., 2015).

As an analogy, loss of BAK1 is like losing the “fuel” of apoptosis (i.e., apoptosis attenuation). Turning off apoptosis effectors is an effective strategy to proactively evade apoptosis, and we show eliminating BAK1 is essential for this purpose in neurons. Regulation of other effectors (e.g., caspases) is likely as important but simultaneously constrained by their non-apoptotic functions (e.g., axon pruning, etc.). The genetic necessity of apoptosis attenuation for animal survival is clearly demonstrated by $Bak1^{\Delta exon5/+}$ mice, which remove the natural BAK1 “knockout” in neurons. While prevailing thought emphasizes the necessity of apoptosis during development, our study shows that apoptosis attenuation is as essential to brain function and animal survival.

## STAR METHODS

### Lead Contact

Further information and requests for resources and reagents should be directed to and will be fulfilled by the Lead Contact, Sika Zheng (sikaz@ucr.edu).

### Materials Availability

All the reagents generated in this study are available from the Lead Contact without restriction or with a completed Materials Transfer Agreement.

### Data and Code Availability

The RNA-Seq data for E12 neocortices generated in this study is available at NCBI GEO: GSE149491.

RNA-Seq data for E14, E17, P2 neocortices (NCBI GEO: GSE84803) and RNA-Seq data for mouse embryonic stem cell differentiation (NCBI GEO: GSE71179) are available from NCBI GEO.

Human embryonic stem cell differentiation data (ENCFF000FCX, ENCFF585VNQ, ENCFF509QEV) is available from the ENCODE Consortium.

Source data for Figure 3A in this paper is available at http://www.gtexportal.org/home/gene/BAK1.

Original data for Figure 3H in this paper is available at Human Proteome Map project: https://www.humanproteomemap.org.

## EXPERIMENTAL MODEL AND SUBJECT DETAILS

### Mice

All mice were maintained and used for experiments according to the requirements of the Institutional Animal Care and Use Committees (IACUC) at the University of California, Riverside. Under routinely monitoring and checking of veterinary and mouse room staff, all animals used in this study were kept healthy in a mouse room with a stable temperature at 22±2°C and a 12h light/dark cycle. Ventilated cages and clean bedding were changed every two weeks. Food and water were provided ad libitum. No more than 5 mice were allowed in each cage. The *Upf2*$^{loxp/loxp}$ mice were described previously (Zheng et al., 2012). *Emxi-Cre* $^{+/-}$ mice were purchased from the Jackson Laboratory and bred with *Upf2*$^{loxp/loxp}$ mice to generate *Upf2* conditional KO mice. C57BL/6J mice were obtained from the Jackson Laboratory and bred for time pregnancy. Time pregnant CD-1 (ICR) mice were ordered from Charles River Hollister. The *Bak1*$^{\Delta E5/+}$ mice were generated in West Virginia University. Briefly, we targeted the *Bak1-exon5* gene by CRISPR/Cas9 system at both intron4 site (GTCTGCGTCATGCGTCTGCG) and intron6 site (TAGCCGTGTAGCTTCCCATC). The gRNAs and Cas9 proteins were purchased from Synthego and *in vitro* assembled into two separate RNPs, which were co-electroporated into C57BL/6J zygotes. Electroporated embryos were cultured for a day and transferred into foster dams. F0 pups were screened by PCR genotyping for founders with an exon 5 deletion allele. Genotyping primers: (F1-TAGAACAGCTTCAGCCCACA; R1-CCCAGCTGATGCCACTCTTA; F2-GCAGGCGGCAAGTTTAAGTA; R2-AGAGGGAAGAGCGACCAGAT). All founders, two from the first CRISPR targeting trial and four from the second CRISPR trial, were genetically-mosaic. Founders were crossed with C57BL/6 WTs to obtain heterozygous mutants. Data on the exon 5 deletion mutant were collected from heterozygous (and WT) offspring of these six founders. Data from different founders showed the same phenotypes of heterozygous mutants. All the mouse maintenance and experiments were approved by and performed in accordance with the guidelines by the Institutional Animal Care and Use Committee of the University of California, Riverside.

### Mouse cortical neural progenitor cells

Primary cortical neurosphere and neural progenitor cell culture was performed as described previously (Frappart et al., 2005). The mouse neocortices at E14 were collected and digested in 1 X TrypLE Express (Invitrogen/Gibco) at 37°C for 15–20 minutes. Neurospheres were cultured in neural stem cell medium containing DMEM-F12 (Invitrogen/Gibco), 1 X B27 (Invitrogen/Gibco), 1 X GlutaMAX (Invitrogen/Gibco), 20 ng/ml EGF (Peprotech) and 20 ng/ml β-FGF (Peprotech) for 5–7 days in T25 flask. Then neurospheres were dissociated in 1 X TrypLE Express and extendedly cultured in T75 flask for another 5–7 days. After that, neural progenitor cells were plated on dishes or plates, pre-coated with 50 μg/ml

polyornithine (Sigma) and 1 μg/ml fibronectin (Sigma) for 2 h at 37°C. Cortical neural progenitor cells were usually passaged twice or thrice to get rid of the clusters before experiments. For immunostaining, neural progenitor cells were plated at 100,000 / well in 24-well plate and collected at 24 hours; for immunoblotting, neural progenitor cells were plated at 1000,000 / well in 6-well plate or 35 mm dish and collected at 24 hours.

### Mouse cortical primary neuron culture

Primary cortical neuron culture was conducted as reported before (Zheng et al., 2010). Concisely, the E14 mouse neocortices were dissected and digested in 0.25% trypsin (Thermo Fisher Scientific) containing 1mM EDTA (Sigma) and 1 X HBSS (Invitrogen) at 37°C for 8–10 minutes. After digestion, cortical neurons were dissociated in plating media containing MEM (Invitrogen/Gibco), 20% heat-inactivated horse serum (Life Technologies), 25 mM glucose (Sigma) and 1 X GlutaMAX (Invitrogen/Gibco). Then cortical neurons were centrifuged and resuspended in fresh plating media without trypsin, and then plated on dishes or plates, pre-coated with 0.1 mg/ml poly L-lysine (Sigma) and 5 μg/ml Laminin (Thermo Fisher Scientific). Six hours later, cortical neurons were cultured in feeding media containing Neurobasal (Invitrogen/Gibco), 1 X B27 (Invitrogen/Gibco) and 1 X GlutaMAX (Invitrogen/Gibco). For maintenance, feeding media were changed for a half volume every three to four days. For Cycloheximide (CHX, Fisher Scientific) treatment, the concentration of 0.5 mg/ml was used for 5 hours before collecting for RNA extraction. For immunostaining, cortical neurons were plated at 100,000 / well in 24-well plate and collected at the desired time points; for immunoblotting, neurons were plated at 1000,000 / well in 6-well plate or 35 mm dish and collected at the desired time points.

### Cell culture and treatments

Neuro-2a cells were maintained in DMEM media containing 10% FBS (Invitrogen) and 1 X GlutaMAX (Invitrogen/Gibco). For siRNA knockdown experiments, Lipofectamine RNAiMax (Life Technologies), Silencer Select siRNAs (siPtbp1#1-s72335, siPtbp1#2-s72336 and siPtbp2#1-s80148, Life Technologies) and Silencer Negative Control siRNA (siCtr-AM4615, Life Technologies) were used right after plating cells at 200,000 per well in 6-well plates according to the manufacturer's instruction. For apoptotic assay, 0.5 μM Staurosporine (Sigma) was given for 5 hours in the media before collecting cells. For primary neurons or neural progenitors, 0.5 μM Staurosporine was given for 5 hours in their feeding media before collecting or fixing them. Caspase inhibitors as Z-VAD-FMK or Z-DEVD-FMK (Selleckchem) were administrated at 50 μM together with Staurosporine for 5 hours before fixing them. For minigene reporter transfection, Lipofectamine 2000 (Life Technologies) was used in transient transfection for pFlare9A constructs according to the manufacturer's protocol. Moreover, in Ptbp1 knockdown group, the pFlare9A constructs were co-transfected with psi-shPTBP1 at the ratio 1:3 for 48 hours. All the cells were transfected for 48 hours before harvesting for RNA extraction, immunoblotting or immunostaining according to experiments. For each biological replicate, DMSO and STS treatment were conducted at the same time on the same batch of NPC cultures with the same plating density (50,000 cells / $cm^2$). The same process was applied to experiments on primary neuronal cultures. NPCs and neurons were plated the same density and images were taken in an unbiased manner without field selection. Because the cultures were not

confluent, some fields appeared denser than others. For quantification, 5 or 6 images were taken per well; 3 or 4 wells were counted per biological replicate; and three biological replicates were included in the quantification plot.

### Sex as a biological variable

We monitored the possible influence of sex on our findings generated from the *Bak1* mutant and *Upf2* conditional knockout mice. We observed no influence of sex on AS-NMD regulation of *Bak1* or the mouse phenotypes.

## METHOD DETAILS

### Immunofluorescent staining of cortical progenitors and primary cortical neurons

Mouse cortical progenitors and primary neurons were plated on glass coverslips (Thermo Fisher Scientific), pre-coated with coating media mentioned before and maintained in each culture media. After treatment or at a desired time point, cells were washed with cold PBS twice, fixed with 4% PFA for 15–20 min at room temperature and then rinsed with PBS three times. Later, cells were permeabilized in PBS containing 0.3% Triton X-100 for 10 min, and then incubated in blocking buffer (5% Donkey serum, 1% BSA and 0.1% Triton X-100 in pH7.4 PBS) for one hour. After that, cells were incubated in blocking buffer diluted primary antibody solution, as rabbit anti-Cleaved Caspase3 (CST#9661, 1:500), mouse anti-NeuN (Millipore#MAB377, 1:800), mouse anti-Nestin (Millipore#MAB353, 1:800), chicken anti-Map2 (Abcam#ab5329, 1:4000), mouse anti-Tau1–1 (Millipore#MAB3420, 1:1000), at 4°C overnight. On the second day, cells were washed with PBS containing 0.1% Triton X-100 (PBST) for three times, and then incubated with appropriate Alexa Fluor secondary antibodies (Life Technologies, 1:1000) diluted in PBST for one hour at room temperature. After staining with DAPI (1:500 diluted in PBS) for 10 min, cells were rinsed with PBS three times and mounted with ProLong Gold Antifade Mountant (Thermo Fisher Scientific). Images are taken and quantified on a Nikon Eclipse Ci microscope with NIS-Elements BR4.5 software, or on Zeiss LSM800 with ZEN software.

### PTBP1-overexpressed stable cell lines

For generating PTBP1-overexpressed stable cell lines, the PTBP1 plasmid carrying GFP was transfected transiently into Neuro-2a cells for 48 hours. Then the cells were dissociated and sorted by the flow cytometry to get the single $GFP^+$ cell in each well of the 96-well plate. When the wells were confluent with $GFP^+$ cells, trypsinize and transfer into 24-well plates. Furthermore, the cells were sorted again using the flow cytometry when the wells were confluent with $GFP^+$ cells in 6-well plates. Then the $GFP^+$ cells were maintained in Neuro-2a medium and the protein samples were collected after several generation to verify the overexpression of Flag-PTBP1 using western blotting.

### Apoptotic analysis by flow cytometry

FITC Annexin V Apoptosis Detection Kit (BD#556547) was used to detect the apoptotic Neuro-2a cells treated with 0.5 μM Staurosporine for 5 hours. Based on the manufacturer's instructions, siPtpb1 and siCtr transient knockdown was conducted at 200 K per well for 6-well plates and cultured for 43 hours before Staurosporine treatment. After 5 h treatment, the

cells were dissociated with 0.25% Trypsin and washed twice with cold PBS. Then, 1 X Binding buffer was used to resuspend cells at the concentration around 1 X $10^6$ / ml. Furthermore, 100 μl cell suspension was transferred to a new 1.5 ml Eppendorf tube and 2.5 μl FITC-Annexin V and 2.5 μl PI solutions were added into each tube for 15 min incubation at room temperature in the dark. After that, 200 μl 1 X Binding buffer was added into each tube. Lastly, NovoCyte Flow Cytometer (ACEA Biosciences) was used to detect both early apoptotic cells labelled with FITC only and late apoptotic cells labelled with both FITC and PI. Unstained Neuro-2a cells were used as negative control. Cells stained with FITC-Annexin V only and cells stained with PI only were used for the fluorescent compensation.

### Protein extraction and immunoblotting

Proteins were extracted from brain tissues, cortical neuroprogenitor cells, primary cortical neurons and Neuro-2a cells in RIPA buffer containing 50 mM Tris HCl pH 7.4, 150 mM NaCl, 1% Triton X-100, 0.1% SDS, 0.2 μl/ml Benzonase Nuclease (EMD Millipore) and 1X EDTA-free protease inhibitor cocktail (Roche). Protein lysate was collected by centrifuging at 14,800 rpm for 20 minutes at 4°C to get rid of the insoluble residue. Pierce BCA protein assay kit (Thermo Fisher Scientific) was used to detect the concentration, and then protein samples were normalized and inactivated with 4X Laemmli sample buffer (Bio-Rad) containing 10% β-mercaptoethanol at 95°C for 10 minutes. For immunoblotting, run the linear SDS-PAGE, and Immobilon-FL PVDF membrane (Millipore) were blotted and stained with primary antibodies in TBST containing 1–5% non-fat dried milk, followed by incubation with fluorescent conjugated secondary antibodies and detected using the Typhoon FLA9000. For the primary antibodies, we used rabbit anti-PTBP1 (Douglas Black Lab, 1:1000), rabbit anti-PTBP2 (Douglas Black Lab, 1:2000), rabbit anti-cleaved Capase3 (CST#9661, 1:400), mouse anti-GAPDH (Ambion#4300, 1:2000) and rabbit anti-Flag (Sigma#F7425, 1:1000). For the secondary antibodies, we used Alexa Fluor 488 donkey anti-rabbit (Invitrogen#21206, 1:1000) and Alexa Fluor 647 donkey anti-mouse (Invitrogen#31571, 1:1000). For rabbit anti-BAK1 (Millipore#06–536, 1:400) primary antibody, horseradish peroxidase (HRP)-conjugated secondary antibody and ECL reagents (Thermo Fisher Scientific) were used to develop the PVDF membrane. The band intensities were analyzed from at least three biological replicates and quantified by ImageQuant TL and ImageJ softwares and the statistical analysis was carried out using Microsoft Excel.

### RNA extraction and Real-time quantitative PCR (RT-qPCR)

According to the manufacturer's protocol, total RNA was extracted from brain tissues, cortical neuroprogenitor cells, primary cortical neurons and Neuro-2a cells using TRIzol reagent (Thermo Fisher Scientific). Then Turbo DNase (Ambion) was used to get rid of the DNA contamination in RNA samples before cDNA synthesis. M-MLV reverse transcriptase (Promega) was used to synthesize the first-strand cDNAs with random hexamers and the total volume of RNA input for each reaction was 1 μg. For RT-qPCR, 10 μl reaction was conducted using a Quantstudio 6 Real-Time PCR instrument, containing 0.3 μl 1:10 diluted cDNA, 5 μl 2X SYBR Green PCR master mix (Life Tech), 0.3 μM forward and reverse primers. The primer sequences were as follows: *Bak1-E5*$^{-}$ 5'-GATATTAACCGGCGCTACGA-3' and 5'-GCCACTCTTAAATAGGCTGGA-3'; *Bak1-E5*$^{+}$ 5'-AGCAGCAACATGCACAGC-3' and 5'-GGTAGACGTACAGGGCCAGA-3'; *Bak1-*

exon1intron1 5’-CCACATCTGGAGCAGAGTCA-3’ and 5’-GTTGCCGATGGAGGTTTCT-3’; *Gapdh* 5’-TGCGACTTCAACAGCAACTC-3’ and 5’-CTTGCTCAGTGTCCTTGCTG-3’. *Sdha* 5’-GCTTGCGAGCTGCATTTGG-3’ and 5’-CATCTCCAGTTGTCCTCTTCCA-3’; *Hprt* 5’-AGCTACTGTAATGATCAGTCAACG-3’ and 5’-AGAGGTCCTTTTCACCAGCA-3’.

### RT-PCR, Minigene reporter and QIAxcel quantitative capillary electrophoresis analysis

For QIAxcel analysis as described previously (Zhang et al., 2019), the RT-PCR was conducted with 6 μl 1:10 diluted cDNA, 0.25 μM forward and reverse primers, and Taq DNA polymerase (New England Biolabs) following the manufacturer’s instructions. Thermo-cycler conditions were as follows: 94°C at 4 min for 1 cycle; 94°C 15 s, 60°C 30 s, 72°C 30 s for 27 cycles; 72°C at 5 min for 1 cycle. Primer sequences were listed below: RT-PCR primer sequences for endogenous *Bak1*: 5’-TAGAACAGCTTCAGCCCACA-3’ and 5’-CCCAGCTGATGCCACTCTTA-3’. For the primer sequences targeting the differentiated-splicing exons during development, see Table S4. PCR primer sequences for *Bak1-E5* WT construct cloning: 5’-CCGGAATTCCTCTTCTGTCCTTTTCTCTCTG-3’ and 5’-GCGGGATCCTGAGAGGGAAGAGCGACCA-3’; and *Bak1-E5* Mut construct cloning: 5’-CCGGAATTCTTTTTCTGTTCTTTTTTTTCTG-3’ and 5’-GCGGGATCCTGAGAGGGAAGAGCGACCA-3’. *Bak1-E5* WT and Mut constructs were cloned into the pFlare-9A at EcoRl and BamHl sites with standard cloning techniques. RT-PCR primer sequences for the minigenes were 5’-CGTCGCCGTCCAGCTCGACCAG-3’ and 5’-AGATCTACCATTGGTGCACCTGA-3’. Subsequently, the capillary electrophoresis analysis on the QIAxcel System (Qiagen) was used to load the RT-PCR amplicons on a QIAxcel DNA cartridge (Qiagen) and then to run side by side with a 25–500 bp DNA size marker (Qiagen) as per manufacturer’s instructions. Imaging and statistical analysis of RT-PCR products were conducted by QIAxcel ScreenGel software, and then come out as Microsoft Excel.

### *In Utero* Electroporation

According to the protocol described previously (Saito, 2006), the E14.5 time-pregnant mouse was anesthetized with vaporized isoflurane, which mixed ahead with air (2:1) in the chamber. Then the mouse was transferred to the warm operating heat pad with a mask of continuous isoflurane mixed with air, and 5 mg / kg Carprofen (Sigma) were given by intraperitoneal injection before surgery. Firstly, one side of the utero was taken out after cutting the midline of the abdominal wall and immersed in warm saline with 1X Pen/Strep antibiotics (Thermo Fisher Scientific). Further, endo-free pCAGIG-PTBP1 or pCAGIG plasmid DNA (1–1.5 μg) mixed with 0.05% Fast Green Dye (Sigma) was microinjected into the lateral ventricles of brain using glass micropipettes (VWR International). The forceps-type electrodes, parallel to the embryonic anteroposterior axis, were used to deliver five electric pulses with every second and a duration of 50 ms per pulse at the voltage 40–42 V using an electroporator (BTX, ECM 830). For the other side of the embryos, we use the same procedure. Afterwards, all embryos were back and warm saline with antibiotics was added into the abdominal cavity. Finally, the abdominal wall and skin were closed with surgical suture. The surgical mice were monitored on the heat pad until they recovered from

the anesthetic. Four days later at E18.5, the brains of the surgical mice would be dissected out and further analyzed by immunofluorescent staining.

## Mouse Brain Sectioning, Immunofluorescence and Immunohistochemistry Staining

Mouse brains were dissected out at desired stages and fixed in 4% PFA at 4°C for 2–14 hours depends on stages. Fixed brains were washed for three times with pH7.4 PBS, embedded in 3% agarose gel and sectioned to 100–150μm using a Vibratome LEICA VT1000 S (Leica). For staining, mouse brain sections were rinsed for three times with PBS, permeabilized with 0.5% Triton X-100 in PBS for half an hour at room temperature, incubated in blocking buffer (10% donkey serum, 2% BSA, 0.3% Triton X-100 in pH7.4 PBS) for 60 min. After blocking, sections were incubated with primary antibody in blocking buffer at 4°C overnight. The primary antibodies were used as follows: mouse anti-BAK1 (Calbiochem#AM04, 1:100), rabbit anti-cleaved Caspase-3 (CST#9661, 1:400), rabbit anti-Flag (Sigma#F7425, 1;100), chicken anti-GFP (Aves#1020, 1:500), rabbit anti-Pax6 (BioLegend#901301, 1:400), mouse anti-Pax6 (BD Biosciences#561664, 1:100), mouse anti-NMDAR2B (BD Biosciences#610416, 1:200), mouse anti-NeuroD2 (Santa Cruz#sc-365896, 1:50), mouse anti-Satb2 (Abcam#51502, 1:400), rabbit anti-PTBP2 (Douglas Black Lab, 1:500). For immunofluorescent staining, sections were rinsed with 0.3% Triton X-100 in PBS twice and treated with appropriate Alexa Fluor conjugated secondary antibodies (Invitrogen, 1:1000) at 4°C overnight on the second day. Next day after staining with DAPI diluted in PBS (1:500) for 30 min at room temperature, sections were washed three times in PBS and mounted with ProLong Gold Antifade Mountant (Thermo Fisher Scientific). For immunohistochemistry staining, sections were rinsed with 0.3% Triton X-100 in PBS twice and treated with endogenous peroxidase blocking (1.5% $H_2O_2$, 20% methanol, 0.3% Triton X-100 in PBS) for half an hour at room temperature, then washed with PBST twice again and finally incubated with HRP conjugated goat anti-Rabbit secondary antibody (Thermo Fisher Scientific, 31466, 1:250) in blocking buffer at 4°C overnight. On the third day, a series washing was carried out (0.3% Triton X-100 in PBS thrice, half an hour each time; twice $H_2O$ washing, 15 minutes each). And then sections were incubated with DAB solution (Vector Laboratories, SK-4100) for 5 minutes. DAB staining was stopped by washing three times with $H_2O$. Afterwards, sections were washed three times in PBS, mounted on glass slide, dehydrated in ethanol gradient, clear with toluene for one hour and mounted with Permount (Thermo Fisher Scientific, SP15–100). The R&D Systems anti-Rabbit HRP-DAB Cell & Tissue Staining Kit (Thermo Fisher Scientific, CTS005) was used for BAK1 (Thermo Fisher Scientific, 06–536-MI) and PTBP1 (Douglas Black Lab) staining according to the vendor's manual with following modifications for thick floating sections: 30 minutes for each washing and peroxidase blocking, 90 minutes for avidin and biotin blocking, 4°C overnight for both primary and secondary antibodies, 60 minutes for HSS-HRP incubation. Images were taken on Eclipse TS100 (Nikon) or LSM800 (Zeiss). Fluorescent Intensity and Positive cell counting were analyzed with NIS-Elements BR4.5 software or ZEN software.

## RNA-Seq analysis

GO terms associated with each gene were downloaded from the Ensembl biomart. There are 1821 genes associated with the GO term "GOC:mtg_apoptosis", collectively termed

apoptosis genes for brevity. These genes contain 1430 annotated cassette exons (middle exons included in some but not all transcript isoforms) based on the mouse GENCODE annotation (mmv20). We used STAR to align reads to the mouse reference genome (GRCm38) and obtained junction read counts. Percent-spliced-in (PSI) is defined as follow: 0.5 x inclusive junction reads / (0.5 x inclusive junction reads + exclusive junction reads) x 100. For ENCODE mouse adult tissues (generated by Thomas Gingera's lab), we retained alternative exons passing the coverage threshold (inclusive junction read count ≥20 or exclusive junction read count ≥10) for a majority of samples (27 out of 32, 84.4%) and with ≤2 missing data values (zero junction read for a sample). A total of 751 alternative exons remained after this filter and were considered in the following analysis. Hierarchical clustering with complete linkage based on Euclidean distances for PSI of alternative exons was performed using R. The missing data (e.g., dropout events) consisting 0.12% of the data points were imputed by the average inclusion ratio across other samples. Mouse developmental forebrain data were downloaded from GSE84803 (Vuong et al., 2016b). E12 forebrain data (GSE149491) was generated with the same procedure at the same time as GSE84803. Alternative exons passing the coverage threshold for all four time points (E12, E14, E17, P2) were considered (1152 alternative exons). For ENCODE mouse developmental midbrain data (generated by Barbara Wold's lab), we combined the reads from the two biological replicates for each time point. We retained alternative exons (a total of 1051) passing the coverage threshold (stated above) for at least 7 out of 8 time points and without any missing data. The hierarchical trees based on the developmental splicing profiles were cut into five (Fig. 1B) and four (Fig. S1C) clusters. The RNA-seq data of developing mouse brain contains four time points for the forebrain and eight time points for the midbrain. For each cluster, we calculated the average PSI at each time point. A regression line was fit between the average PSI and the order of time points (coded as 1, 2, 3, 4 for the forebrain, and 1, 2, 3, 4, 5, 6, 7, 8 for the midbrain). If the slope coefficient is statistically significant ($P \leq 0.05$) and large enough (absolute value ≥ 5 PSI), the exon cluster is declared developmentally-programmed. Junction read counts for human GTEx tissues were downloaded from the GTEx portal and the PSI of BAK1 was calculated and shown for samples passing the coverage threshold. RNA-Seq data from Illumina Human Body Map 2.0 project were downloaded from http://www.ensembl.info/2011/05/24/human-bodymap-2–0-data-from-illumina/. RNA-seq data for the developing human cerebral cortex across different time points (late 8, 9, 10, …17 post conception weeks) were downloaded from https://www.ebi.ac.uk/arrayexpress/experiments/E-MTAB-4840/. Samples belonging to the same time point were combined to achieve an average sequencing depth of ~210 million mapped reads.

## QUANTIFICATION AND STATISTICAL ANALYSIS

Common practices of applying statistical analysis in biological data were applied. For most data, we used two-tailed Student's t-test unless otherwise specified in the figure legends. For the animal survive curve, we used the Log-rank (Mantel-Cox) test in the Prism software. Experimental numbers "N" and what they represent can be found in figure legends.

## Supplementary Material

Refer to Web version on PubMed Central for supplementary material.

## ACKNOWLEDGMENTS

We thank Cheryl Stork for assistance with the design of *Bak1* sgRNAs. We thank Amanda Xaypraseuth and Sarah Easow for technical supports of genotyping and tissue sectioning. We thank Fatimah Matalkah for genotyping and care of the founders. This work was supported by the NIH grants R01MH116220 and R01NS104041 (to S.Z.), R01GM137428 to (L.C.), and R01EY025536 (to P.S.).

## REFERENCES:

Annis RP, Swahari V, Nakamura A, Xie AX, Hammond SM, and Deshmukh M (2016). Mature neurons dynamically restrict apoptosis via redundant premitochondrial brakes. FEBS J. 283, 4569–4582. [PubMed: 27797453]

Barbosa-Morais NL, Irimia M, Pan Q, Xiong HY, Gueroussov S, Lee LJ, Slobodeniuc V, Kutter C, Watt S, Colak R, et al. (2012). The evolutionary landscape of alternative splicing in vertebrate species. Science 338, 1587–1593. [PubMed: 23258890]

Benn SC, and Woolf CJ (2004). Adult neuron survival strategies--slamming on the brakes. Nat. Rev. Neurosci. 5, 686–700. [PubMed: 15322527]

Boutz PL, Stoilov P, Li Q, Lin C-H, Chawla G, Ostrow K, Shiue L, Ares M Jr, and Black DL (2007). A post-transcriptional regulatory switch in polypyrimidine tract-binding proteins reprograms alternative splicing in developing neurons. Genes Dev. 21, 1636–1652. [PubMed: 17606642]

Chang Y-F, Imam JS, and Wilkinson MF (2007). The nonsense-mediated decay RNA surveillance pathway. Annu. Rev. Biochem. 76, 51–74. [PubMed: 17352659]

Chipuk JE, Moldoveanu T, Llambi F, Parsons MJ, and Green DR (2010). The BCL-2 family reunion. Mol. Cell 37, 299–310. [PubMed: 20159550]

Conze DB, Albert L, Ferrick DA, Goeddel DV, Yeh W-C, Mak T, and Ashwell JD (2005). Posttranscriptional downregulation of c-IAP2 by the ubiquitin protein ligase c-IAP1 in vivo. Mol. Cell. Biol. 25, 3348–3356. [PubMed: 15798218]

Czabotar PE, Lessene G, Strasser A, and Adams JM (2014). Control of apoptosis by the BCL-2 protein family: implications for physiology and therapy. Nat. Rev. Mol. Cell Biol. 15, 49–63. [PubMed: 24355989]

Davies AM (1998). Developmental changes in the neurotrophic factor survival requirements of peripheral nervous system neurons. Prog. Brain Res. 117, 47–56. [PubMed: 9932399]

Deckwerth TL, Elliott JL, Knudson CM, Johnson EM Jr, Snider WD, and Korsmeyer SJ (1996). BAX is required for neuronal death after trophic factor deprivation and during development. Neuron 17, 401–411. [PubMed: 8816704]

Dekkers MPJ, and Barde Y-A (2013). Programmed Cell Death in Neuronal Development. Science 340, 39–41. [PubMed: 23559240]

Frappart P-O, Tong W-M, Demuth I, Radovanovic I, Herceg Z, Aguzzi A, Digweed M, and Wang Z-Q (2005). An essential function for NBS1 in the prevention of ataxia and cerebellar defects. Nat. Med. 11, 538–544. [PubMed: 15821748]

Furlanis E, and Scheiffele P. (2018). Regulation of Neuronal Differentiation, Function, and Plasticity by Alternative Splicing. Annu. Rev. Cell Dev. Biol. 34, 451–469. [PubMed: 30028642]

Ghosh A, Carnahan J, and Greenberg ME (1994). Requirement for BDNF in activity-dependent survival of cortical neurons. Science 263, 1618–1623. [PubMed: 7907431]

Giorgi C, Yeo GW, Stone ME, Katz DB, Burge C, Turrigiano G, and Moore MJ (2007). The EJC factor eIF4AIII modulates synaptic strength and neuronal protein expression. Cell 130, 179–191. [PubMed: 17632064]

Hamburger V, and Levi-Montalcini R. (1949). Proliferation, differentiation and degeneration in the spinal ganglia of the chick embryo under normal and experimental conditions. J. Exp. Zool. 111, 457–501. [PubMed: 18142378]

Hardwick JM, and Soane L. (2013). Multiple functions of BCL-2 family proteins. Cold Spring Harb. Perspect. Biol. 5.

Harlin H, Reffey SB, Duckett CS, Lindsten T, and Thompson CB (2001). Characterization of XIAP-deficient mice. Mol. Cell. Biol. 21, 3604–3608. [PubMed: 11313486]

Heard KN, Bertrand MJM, and Barker PA (2015). cIAP2 supports viability of mice lacking cIAP1 and XIAP. EMBO J. 34, 2393–2395. [PubMed: 26427758]

Huang EJ, and Reichardt LF (2001). Neurotrophins: roles in neuronal development and function. Annu. Rev. Neurosci. 24, 677–736. [PubMed: 11520916]

Jakobson M, Lintulahti A, and Arumäe U. (2012). mRNA for N-Bak, a neuron-specific BH3-only splice isoform of Bak, escapes nonsense-mediated decay and is translationally repressed in the neurons. Cell Death Dis. 3, e269. [PubMed: 22297299]

Kafasla P, Mickleburgh I, Llorian M, Coelho M, Gooding C, Cherny D, Joshi A, Kotik-Kogan O, Curry S, Eperon IC, et al. (2012). Defining the roles and interactions of PTB. Biochem. Soc. Trans. 40, 815–820. [PubMed: 22817740]

Ke FFS, Vanyai HK, Cowan AD, Delbridge ARD, Whitehead L, Grabow S, Czabotar PE, Voss AK, and Strasser A. (2018). Embryogenesis and Adult Life in the Absence of Intrinsic Apoptosis Effectors BAX, BAK, and BOK. Cell 173, 1217–1230.e17. [PubMed: 29775594]

Keppetipola N, Sharma S, Li Q, and Black DL (2012). Neuronal regulation of pre-mRNA splicing by polypyrimidine tract binding proteins, PTBP1 and PTBP2. Crit. Rev. Biochem. Mol. Biol. 47, 360–378. [PubMed: 22655688]

Kim M-S, Pinto SM, Getnet D, Nirujogi RS, Manda SS, Chaerkady R, Madugundu AK, Kelkar DS, Isserlin R, Jain S, et al. (2014). A draft map of the human proteome. Nature 509, 575–581. [PubMed: 24870542]

Kole AJ, Swahari V, Hammond SM, and Deshmukh M. (2011). miR-29b is activated during neuronal maturation and targets BH3-only genes to restrict apoptosis. Genes Dev. 25, 125–130. [PubMed: 21245165]

Kole AJ, Annis RP, and Deshmukh M. (2013). Mature neurons: equipped for survival. Cell Death Dis. 4, e689. [PubMed: 23807218]

Lareau LF, Inada M, Green RE, Wengrod JC, and Brenner SE (2007). Unproductive splicing of SR genes associated with highly conserved and ultraconserved DNA elements. Nature 446, 926–929. [PubMed: 17361132]

Linares AJ, Lin C-H, Damianov A, Adams KL, Novitch BG, and Black DL (2015). The splicing regulator PTBP1 controls the activity of the transcription factor Pbx1 during neuronal differentiation. Elife 4, e09268.

Lindsay SJ, Xu Y, Lisgo SN, Harkin LF, Copp AJ, Gerrelli D, Clowry GJ, Talbot A, Keogh MJ, Coxhead J, et al. (2016). HDBR Expression: A Unique Resource for Global and Individual Gene Expression Studies during Early Human Brain Development. Front. Neuroanat. 10, 86. [PubMed: 27833533]

Lindsten T, Ross AJ, King A, Zong WX, Rathmell JC, Shiels HA, Ulrich E, Waymire KG, Mahar P, Frauwirth K, et al. (2000). The combined functions of proapoptotic Bcl-2 family members bak and bax are essential for normal development of multiple tissues. Mol. Cell 6, 1389–1399. [PubMed: 11163212]

Lykke-Andersen S, and Jensen TH (2015). Nonsense-mediated mRNA decay: an intricate machinery that shapes transcriptomes. Nat. Rev. Mol. Cell Biol. 16, 665–677. [PubMed: 26397022]

Mao Z, Bonni A, Xia F, Nadal-Vicens M, and Greenberg ME (1999). Neuronal activity-dependent cell survival mediated by transcription factor MEF2. Science 286, 785–790. [PubMed: 10531066]

Markovtsov V, Nikolic JM, Goldman JA, Turck CW, Chou MY, and Black DL (2000). Cooperative assembly of an hnRNP complex induced by a tissue-specific homolog of polypyrimidine tract binding protein. Mol. Cell. Biol. 20, 7463–7479. [PubMed: 11003644]

Matsuda T, and Cepko CL (2004). Electroporation and RNA interference in the rodent retina in vivo and in vitro. Proc. Natl. Acad. Sci. U. S. A. 101, 16–22. [PubMed: 14603031]

McGlincy NJ, and Smith CWJ (2008). Alternative splicing resulting in nonsense-mediated mRNA decay: what is the meaning of nonsense? Trends Biochem. Sci. 33, 385–393. [PubMed: 18621535]

Merkin J, Russell C, Chen P, and Burge CB (2012). Evolutionary dynamics of gene and isoform regulation in Mammalian tissues. Science 338, 1593–1599. [PubMed: 23258891]

Ni JZ, Grate L, Donohue JP, Preston C, Nobida N, O'Brien G, Shiue L, Clark TA, Blume JE, and Ares M Jr (2007). Ultraconserved elements are associated with homeostatic control of splicing regulators by alternative splicing and nonsense-mediated decay. Genes Dev. 21, 708–718. [PubMed: 17369403]

Oppenheim RW (1989). The neurotrophic theory and naturally occurring motoneuron death. Trends Neurosci. 12, 252–255. [PubMed: 2475935]

Paronetto MP, Passacantilli I, and Sette C. (2016). Alternative splicing and cell survival: from tissue homeostasis to disease. Cell Death Differ. 23, 1919–1929. [PubMed: 27689872]

Polydorides AD, Okano HJ, Yang YY, Stefani G, and Darnell RB (2000). A brain-enriched polypyrimidine tract-binding protein antagonizes the ability of Nova to regulate neuron-specific alternative splicing. Proc. Natl. Acad. Sci. U. S. A. 97, 6350–6355. [PubMed: 10829067]

Popp MW-L, and Maquat LE (2013). Organizing principles of mammalian nonsense-mediated mRNA decay. Annu. Rev. Genet. 47, 139–165. [PubMed: 24274751]

Raj B, and Blencowe BJ (2015). Alternative Splicing in the Mammalian Nervous System: Recent Insights into Mechanisms and Functional Roles. Neuron 87, 14–27. [PubMed: 26139367]

Rebbapragada I, and Lykke-Andersen J. (2009). Execution of nonsense-mediated mRNA decay: what defines a substrate? Curr. Opin. Cell Biol. 21, 394–402. [PubMed: 19359157]

Rossbach O, Hung L-H, Schreiner S, Grishina I, Heiner M, Hui J, and Bindereif A. (2009). Auto- and cross-regulation of the hnRNP L proteins by alternative splicing. Mol. Cell. Biol. 29, 1442–1451. [PubMed: 19124611]

Saito T. (2006). In vivo electroporation in the embryonic mouse central nervous system. Nat. Protoc. 1, 1552–1558. [PubMed: 17406448]

Schwerk C, and Schulze-Osthoff K. (2005). Regulation of apoptosis by alternative pre-mRNA splicing. Mol. Cell 19, 1–13. [PubMed: 15989960]

Sharma S, Falick AM, and Black DL (2005). Polypyrimidine tract binding protein blocks the 5' splice site-dependent assembly of U2AF and the prespliceosomal E complex. Mol. Cell 19, 485–496. [PubMed: 16109373]

Singh R, Letai A, and Sarosiek K. (2019). Regulation of apoptosis in health and disease: the balancing act of BCL-2 family proteins. Nat. Rev. Mol. Cell Biol. 20, 175–193. [PubMed: 30655609]

Spellman R, Llorian M, and Smith CWJ (2007). Crossregulation and functional redundancy between the splicing regulator PTB and its paralogs nPTB and ROD1. Mol. Cell 27, 420–434. [PubMed: 17679092]

Sun YF, Yu LY, Saarma M, Timmusk T, and Arumae U. (2001). Neuron-specific Bcl-2 homology 3 domain-only splice variant of Bak is anti-apoptotic in neurons, but pro-apoptotic in non-neuronal cells. J. Biol. Chem. 276, 16240–16247.

Valacca C, Bonomi S, Buratti E, Pedrotti S, Baralle FE, Sette C, Ghigna C, and Biamonti G. (2010). Sam68 regulates EMT through alternative splicing-activated nonsense-mediated mRNA decay of the SF2/ASF proto-oncogene. J. Cell Biol. 191, 87–99. [PubMed: 20876280]

Vuong CK, Black DL, and Zheng S. (2016a). The neurogenetics of alternative splicing. Nat. Rev. Neurosci. 17, 265–281. [PubMed: 27094079]

Vuong JK, Lin C-H, Zhang M, Chen L, Black DL, and Zheng S. (2016b). PTBP1 and PTBP2 Serve Both Specific and Redundant Functions in Neuronal Pre-mRNA Splicing. Cell Rep. 17, 2766–2775. [PubMed: 27926877]

Wang C, and Youle RJ (2009). The Role of Mitochondria in Apoptosis. Annu. Rev. Genet. 43, 95–118. [PubMed: 19659442]

Yan Q, Weyn-Vanhentenryck SM, Wu J, Sloan SA, Zhang Y, Chen K, Wu JQ, Barres BA, and Zhang C. (2015). Systematic discovery of regulated and conserved alternative exons in the mammalian brain reveals NMD modulating chromatin regulators. Proc. Natl. Acad. Sci. U. S. A. 112, 3445–3450. [PubMed: 25737549]

Youle RJ, and Strasser A. (2008). The BCL-2 protein family: opposing activities that mediate cell death. Nat. Rev. Mol. Cell Biol. 9, 47–59. [PubMed: 18097445]

Zhang M, Ergin V, Lin L, Stork C, Chen L, and Zheng S. (2019). Axonogenesis Is Coordinated by Neuron-Specific Alternative Splicing Programming and Splicing Regulator PTBP2. Neuron 101, 690–706.e10. [PubMed: 30733148]

Zheng S. (2016). Alternative splicing and nonsense-mediated mRNA decay enforce neural specific gene expression. Int. J. Dev. Neurosci.

Zheng S. (2020). Alternative splicing programming of axon formation. Wiley Interdiscip. Rev. RNA e1585.

Zheng S, and Black DL (2013). Alternative pre-mRNA splicing in neurons: growing up and extending its reach. Trends Genet. 29, 442–448. [PubMed: 23648015]

Zheng S, Eacker SM, Hong SJ, Gronostajski RM, Dawson TM, and Dawson VL (2010). NMDA-induced neuronal survival is mediated through nuclear factor I-A in mice. J. Clin. Invest. 120, 2446–2456. [PubMed: 20516644]

Zheng S, Gray EE, Chawla G, Porse BT, O'Dell TJ, and Black DL (2012). PSD-95 is post-transcriptionally repressed during early neural development by PTBP1 and PTBP2. Nat. Neurosci. 15, 381–388, S1. [PubMed: 22246437]

## Highlights

- Intrinsic attenuation of apoptosis starts at neuron birth with *Bak1* exon 5 splicing
- *Bak1* exon 5 inclusion induces NMD and unproductive translation of *Bak1* transcripts
- Neural-specific splicing of *Bak1* exon 5 enables cellular longevity of neurons
- Apoptosis attenuation is essential to brain development and animal survival

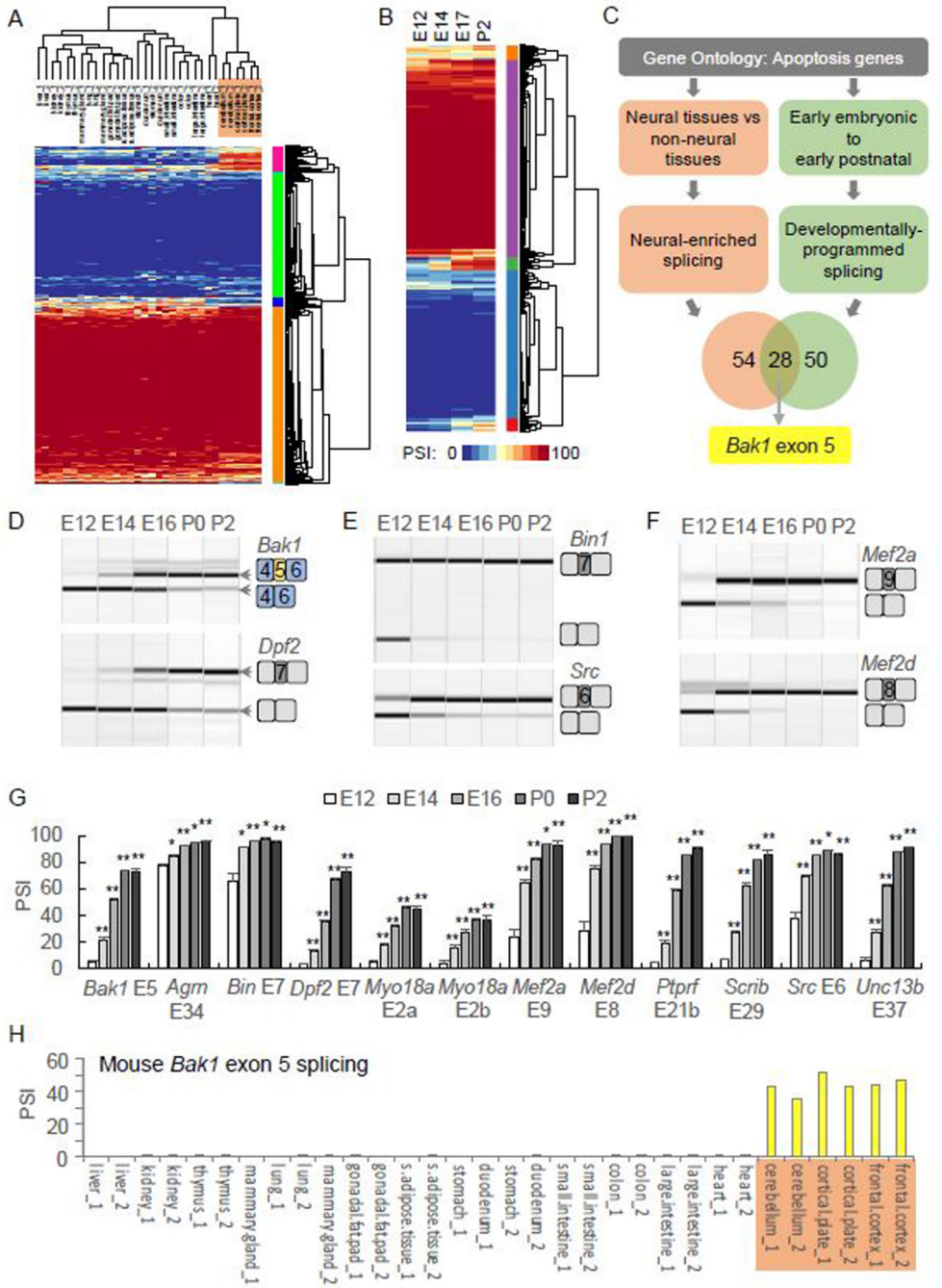


**Figure 1. Neuronal survival is associated with alternative splicing of a subset of apoptosis genes including *Bak1***

(A) Two-way unsupervised hierarchical clustering of alternative exons of apoptosis genes and mouse tissues by percent spliced in (PSI) defines six exon clusters (color coded next to the heatmap). The neural tissues are highlighted in brown. RNA-seq data was obtained from ENCODE (Thomas Gingera's lab).

(B) Unsupervised hierarchical clustering of alternative exons of apoptosis genes by their PSI values in E12, E14, E17 and P2 neocortices defines five exon clusters (color coded next to the heatmap). The third (green) and fifth (red) exon clusters exhibit distinct near-monotonic

splicing changes during development. RNA-seq data was obtained from GSE84803 and GSE149491).

(C) Strategy of identifying alternative exons associated with neuronal survival.

(D-F) Virtual gels of quantitative capillary electrophoresis show splicing changes of apoptosis genes, including *Bak1* and *Dpf2* (D), *Bin1* and *Src* (E), *Mef2a* and *Mef2d* (F) during cortical development from E12 to P2.

(G) Representative neural-specific exons increase splicing in WT (WT) neocortices from E12 to P2. N=5 for E14 and E16; N=4 for E12 and P2; N=2 for P0. Data are represented as the mean ± SEM; *, P<0.05; **, P<0.01; paired Student's t-test for two-tailed distribution with unequal variance.

(H) *Bak1* exon 5 splicing in mouse tissues. The neural tissues are highlighted in brown. See also Figures S1 and S2 and Tables S1-S4.

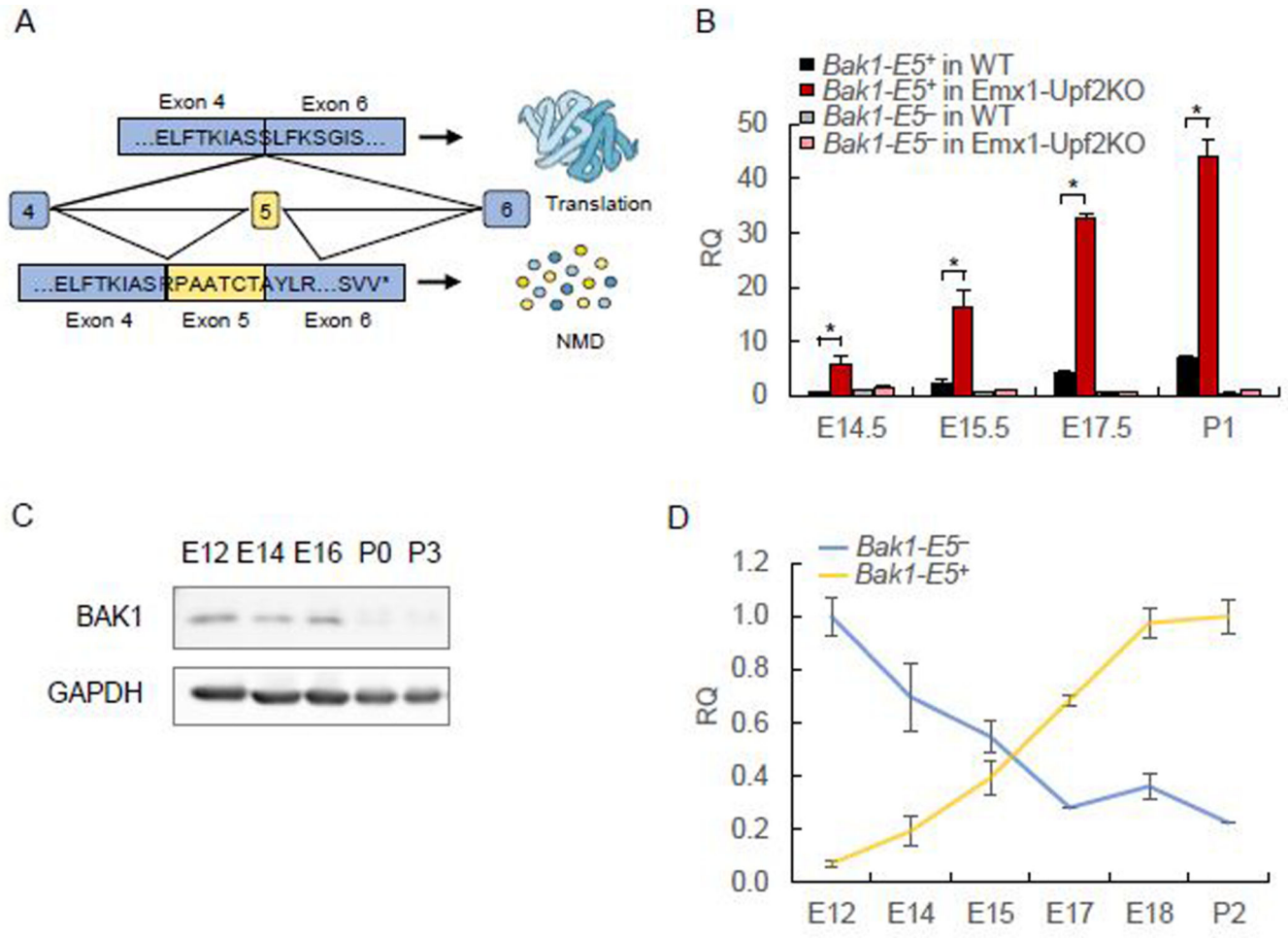


**Figure 2. Exon 5 splicing leads to NMD and unproductive translation of *Bak1* transcripts**

(A) Schematic of AS-NMD regulation in *Bak1* expression. Exon 5 inclusion shifts the reading frame and results in a premature termination codon (*).

(B) RT-qPCR detection of *Bak1* E5$^{-}$ and E5$^{+}$ isoforms in WT and Emx1-Upf2cKO neocortices respectively, from E14.5 to P1. The relative isoform level was normalized to the corresponding isoform in E14.5 WT neocortices. C57BL/6 littermates of WT controls (Upf2$^{loxp/loxp}$) and mutants (Upf2$^{loxp/loxp}$, Emx1-Cre) are from breeding Upf2$^{loxp/loxp}$ with Upf2$^{loxp/+}$, Emx1-Cre mice. N=2–4 for each genotype at each time point. Data are represented as the mean ± SEM; *, P<0.05 and fold change > 2.0; two-tailed Student's t-test with unequal variances.

(C) Western blotting for BAK1 expression in WT neocortices from E12 to P3. Quantification of the Western blot is integrated in Figure 7A.

(D) RT-qPCR detection of both *Bak1* E5$^{-}$ and E5$^{+}$ isoforms in WT CD1 mouse neocortices from E12 to P2. N=2–4 for each time point. *Bak1* E5$^{-}$ relative expression was normalized to the E12. *Bak1* E5$^{+}$ relative expression was normalized to the P2. Data are represented as the mean ± SEM. See also Figure S3 and Table S5.

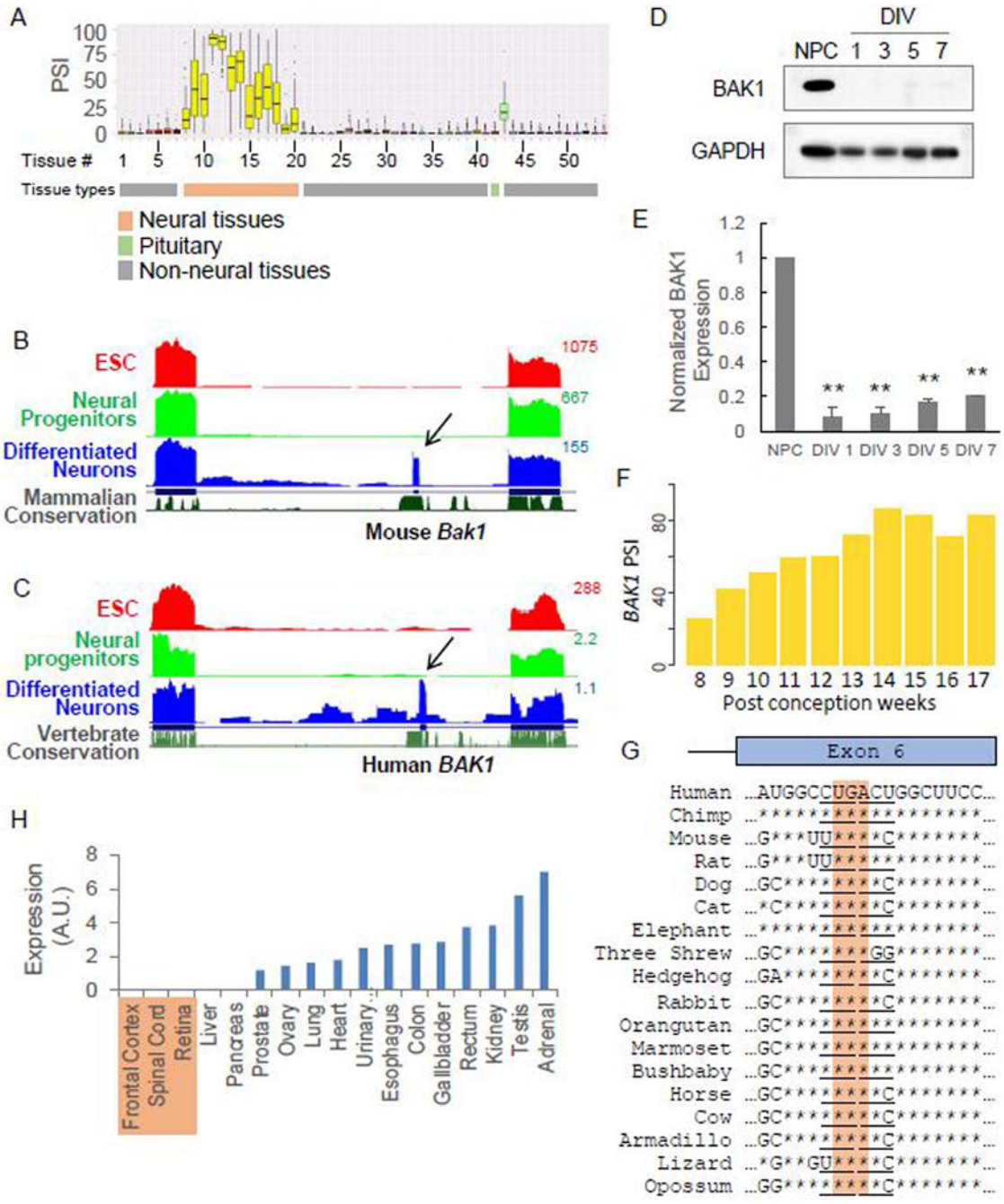


**Figure 3. Developmental regulation of *Bak1* splicing is conserved**

(A) *BAK1* exon 5 splicing in human tissues. Human tissues (GTEx) are alphabetically ordered with tissue #: 1. Adipose-Subcutaneous; 2. Adipose-Visceral (Omentum); 3. Adrenal Gland; 4. Artery-Aorta; 5. Artery-Coronary; 6. Artery-Tibial; 7. Bladder; 8. Brain-Amygdala; 9. Brain-Anterior cingulate cortex (BA24); 10. Brain-Caudate (basal ganglia); 11. Brain-Cerebellar Hemisphere; 12. Brain-Cerebellum; 13. Brain-Cortex; 14. Brain-Frontal Cortex (BA9); 15. Brain-Hippocampus; 16. Brain-Hypothalamus; 17. Brain-Nucleus accumbens (basal ganglia); 18. Brain-Putamen (basal ganglia); 19. Brain-Spinal cord

(cervical c-1); 20. Brain-Substantia nigra; 21. Breast-Mammary Tissue; 22. Cells-EBV-transformed lymphocytes; 23. Cells-Transformed fibroblasts; 24. Cervix-Ectocervix; 25. Cervix-Endocervix; 26. Colon-Sigmoid; 27. Colon-Transverse; 28. Esophagus-Gastroesophageal Junction; 29. Esophagus-Mucosa; 30. Esophagus-Muscularis; 31. Fallopian Tube; 32. Heart-Atrial Appendage; 33. Heart-Left Ventricle; 34. Kidney-Cortex; 35. Kidney-Medulla; 36. Liver; 37. Lung; 38. Minor Salivary Gland; 39. Muscle-Skeletal; 40. Nerve-Tibial; 41. Ovary; 42. Pancreas; 43. Pituitary; 44. Prostate; 45. Skin-Not Sun Exposed (Suprapubic); 46. Skin-Sun Exposed (Lower leg); 47. Small Intestine-Terminal Ileum; 48. Spleen; 49. Stomach; 50. Testis; 51. Thyroid; 52. Uterus; 53. Vagina; 54. Whole Blood. Tissue types are color coded below the graph.

(B-C) Genome browser tracks show *Bak1* (including its exon 5) expression during differentiation of (B) mouse embryonic stem cells (ESC) and (C) human ESCs into neurons. RNA-seq data were obtained from GSE71179 (mouse) and ENCODE (ENCFF000FCX, ENCFF585VNQ, ENCFF509QEV, human), respectively.

(D-E) Western blotting and quantification for BAK1 expression in mouse primary neuronal progenitor cells (NPC) and mouse primary cortical neurons (DIV1 to DIV 7). Data are represented as the mean ± SEM; N=3; **, P<0.01; two-tailed Student's paired t-test.

(F) PSI values of human *BAK1* exon 5 gradually increased in developing brains from 8 to 17 weeks post conception. RNA-seq data were downloaded from https://www.ebi.ac.uk/arrayexpress/experiments/E-MTAB-4840/.

(G) Conservation of the premature termination codon (brown highlight) in the $E5^{+}$ isoform among various species. The codon triplets of all $E5^{-}$ isoform are underscored.

(H) BAK1 protein is undetectable in adult human neural tissues by mass spectrometry (brown highlight). Data compiled from Human Proteome Map project: https://www.humanproteomemap.org. See also Figure S3.

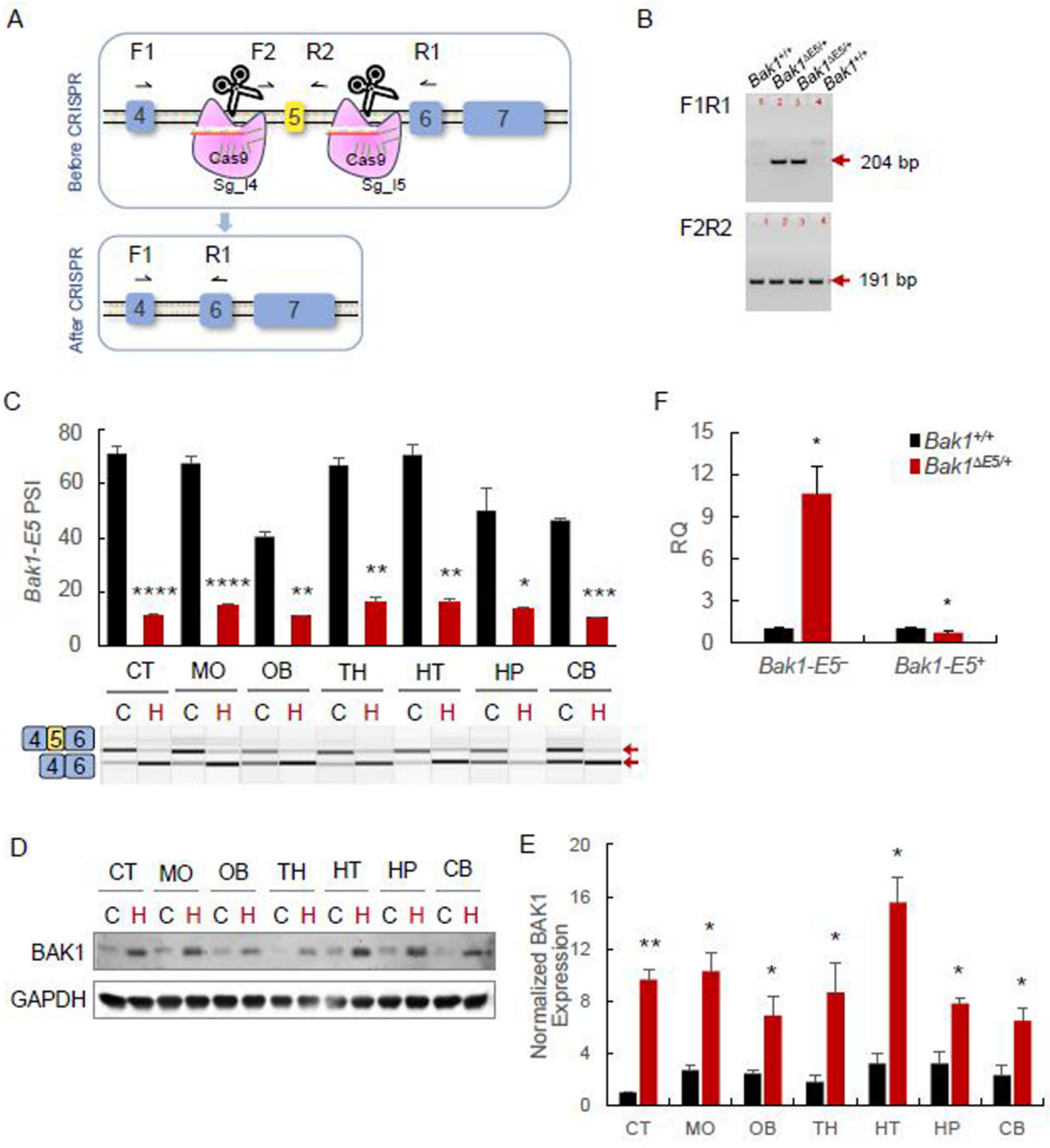


**Figure 4. Heterozygous deletion of *Bak1* exon 5 dis-inhibits BAK1 protein expression in the mouse brain**

(A) Schematic of the CRISPR/Cas9 strategy for the *Bak1-exon5* deleted mouse. Sg_I4 and Sg_I5 denote guide RNA targeting introns 4 and 5. F1, F2, R1, and R2 indicate the positions of genotyping primers.

(B) Genotyping results for the $Bak1^{\Delta exon5/+}$ (or $Bak1^{\Delta E5/+}$) and $Bak1^{+/+}$ mice. F1R1 and F2R2 detect KO alleles (204 bp) and WT alleles (191 bp), respectively. The locations of those primers are shown in (A).

(C) PSI of *Bak1* exon 5 (top) and representative virtual gels (bottom) in various brain tissues of P0 $Bak1^{\Delta E5/+}$ mice (H in red) and their littermate controls (C in black). Data are represented as the mean ± SD of three different litters in Cortex (CT) and Medulla Oblongata (MO) ($N_H$=5, $N_C$=9); ****, P<0.01 × $10^{-11}$; Data are represented as the mean ± SD of two different litters ($N_H$=2, $N_C$=2) in other brain tissues, including Olfactory Bulb (OB), Thalamus (TH), Hypothalamus (HT), Hippocampus (HP) and Cerebellum (CB); *, P<0.05; **, P<0.01; ***, P<0.001; two-tailed Student's paired t-test.
(D-E) Immunoblotting and quantification of the BAK1 expression in P0 $Bak1^{\Delta E5/+}$ (H in red) and $Bak1^{+/+}$ (C in black) brain tissues shown in (C). Data are represented as the mean ± SEM; N=3; *, P<0.05; **, P<0.01; two-tailed Student's paired t-test.
(F) RT-qPCR detection of both *Bak1* $E5^-$ and $E5^+$ isoforms in P0 $Bak1^{\Delta E5/+}$ and $Bak1^{+/+}$ neocortices. Data are represented as the mean ± SEM in three independent litters; N=3; *, P<0.05; two-tailed Student's paired t-test. See also Table S5.

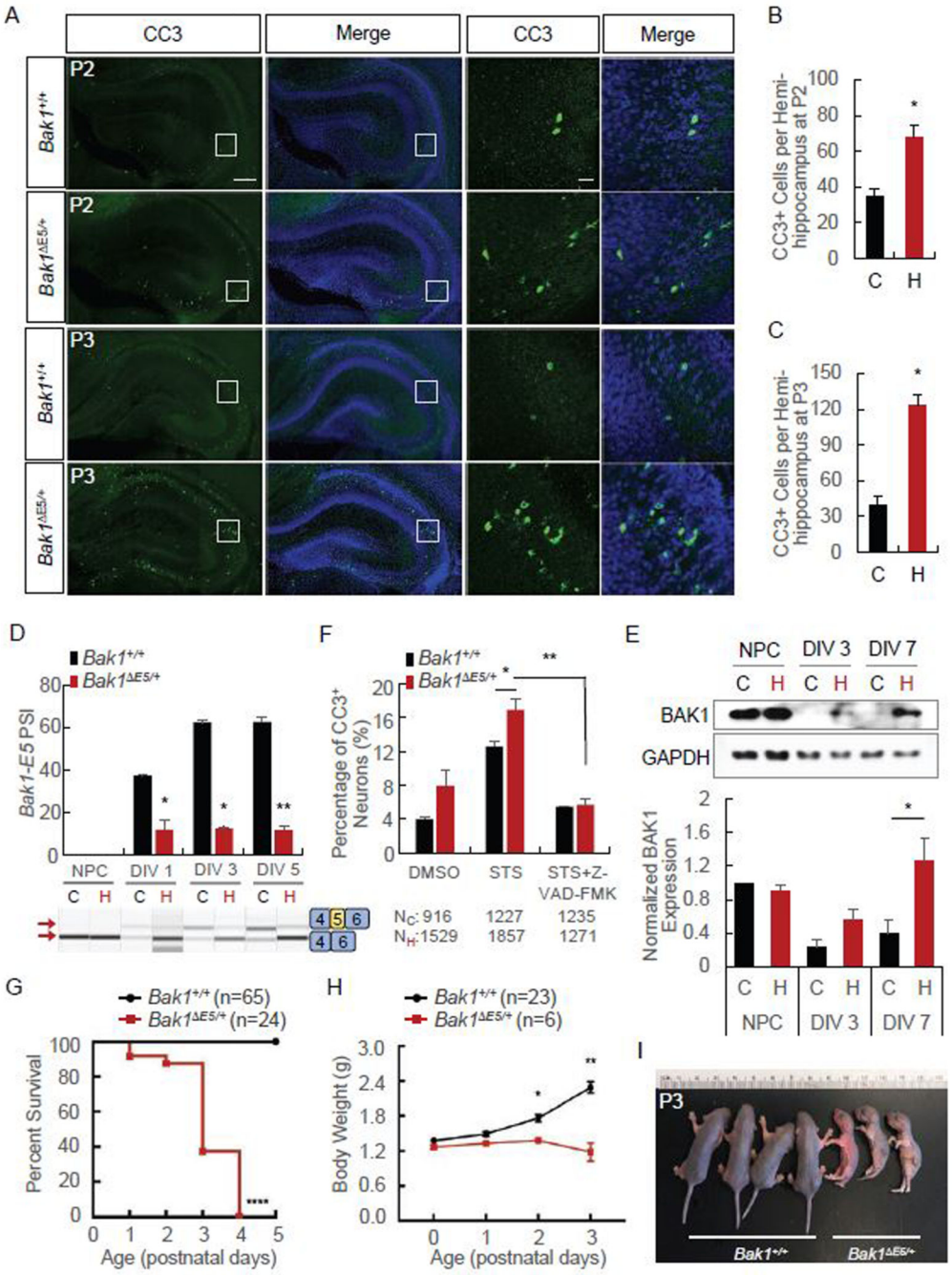


**Figure 5. The phenotypes of *Bak1*$^{\Delta E5/+}$ mice**

(A) Immunofluorescence staining of Cleaved Caspase3 (CC3) in the *Bak1*$^{\Delta E5/+}$ and the *Bak1*$^{+/+}$ hippocampi at postnatal day 2 and 3 (P2 and P3). Those are 2 X 3 tiled images taken by Zen Blue. Scale bars: 200 μm in images of the first two columns and 20 μm in images of the third and fourth columns.

(B-C) Quantification of the number of CC3$^{+}$ cells in hemi-hippocampus per brain slice at P2 and P3. Data are represented as the mean ± SEM. N=3; 4 slices per biological replicate at

each time point and 2 hemi-hippocampus per slice; *, P<0.05; two-tailed Student's paired t-test.

(D) PSI of *Bak1* exon 5 in primary NPC and primary cortical neurons from DIV 1 to DIV 7 in $Bak1^{\Delta E5/+}$ mice (H in red) and their littermate controls (C in black). Data are represented as the mean ± SD of two different litters; N=2; *, P<0.05; **, P<0.01; two-tailed Student's paired t-test.

(E) Immunoblotting and quantification of BAK1 protein expression in cultured cortical NPC, DIV 3 and DIV 7 cortical neurons in $Bak1^{\Delta E5/+}$ mice (H in red) and their littermate controls (C in black). Data are represented as the mean ± SEM of two different litters. N=3; *, P<0.05; two-tailed Student's paired t-test.

(F) Quantitative analysis of $CC3^{+}$ cortical neurons in DIV 5 $Bak1^{\Delta E5/+}$ and the $Bak1^{+/+}$ cortical cultures at 5 hours after 0.5 μM STS treatment with or without 50 μM Caspase inhibitor (Z-VAD-FMK). Data are represented as the mean ± SD of two different litters. N=2; *, P<0.05; **, P<0.01; two-tailed Student's paired t-test.

(G) Survival curves for $Bak1^{\Delta E5/+}$ and littermate control mice. Data are analyzed by Log-rank (Mantel-Cox) test by Prism; $N_H$=24, $N_C$=65; ****, P<0.0001.

(H) Body weights of $Bak1^{\Delta E5/+}$ and littermate control mice. Data are represented as the mean ± SD of five different litters. $N_H$=6, $N_C$=23; *, P<0.05; **, P<0.01; two-tailed Student's paired t-test for each time point.

(I) Image of the $Bak1^{\Delta E5/+}$ pups and their littermate controls at P3. See also Figures S4, S5, S6, and S7.

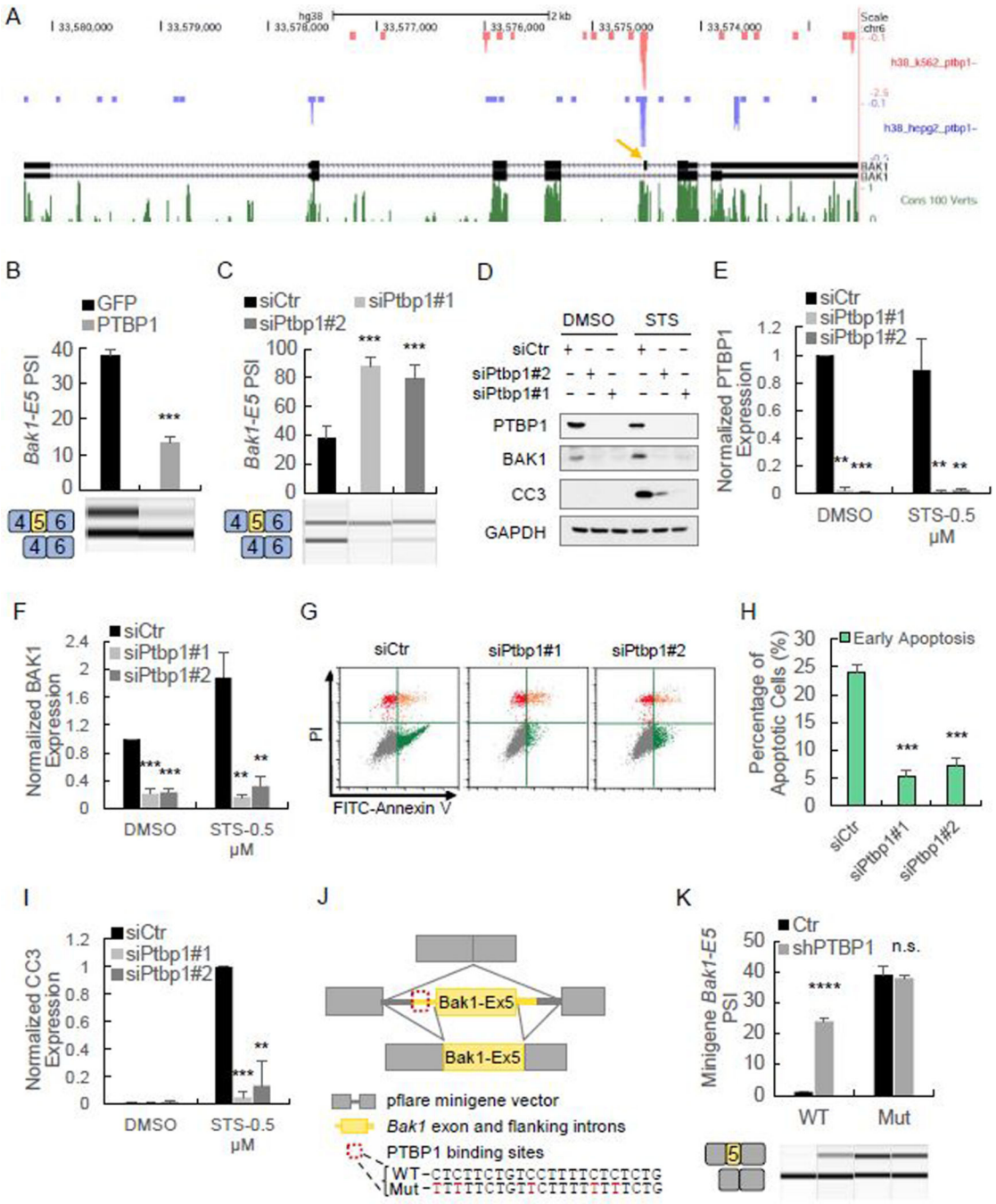


**Figure 6. PTBP1 inhibits *Bak1* exon 5 splicing and modulates apoptotic sensitivity**

(A) Genome browser tracks of PTBP1 eCLIP-Seq in K562 (coral) and HepG2 (blue) cells, *BAK1* gene, and its sequence conservation among 100 vertebrates (phastCons). Data were obtained from ENCODE (ENCFF617YCT for K562 cells and ENCFF936SHU for HepG2 cells). The yellow arrow points to exon 5.

(B) PSI of *Bak1-E5* (top) and representative virtual gels (bottom) in Neuro-2a cells after transient transfection of PTBP1 and GFP control. Data are represented as the mean ± SD of three independent replicates. N=3; ***, p<0.001; two tailed Student's paired t-test.

(C) PSI of *Bak1* exon 5 (top) and representative virtual gels (bottom) in Neuro-2a cells after siRNA-mediated PTBP1 knockdown. Data are represented as the mean ± SD of three independent replicates. N=3; ***, $p<0.001$; two tailed Student's paired t-test.
(D-F) Western blotting for PTBP1, BAK1 and CC3 in siCtr and siPtbp1-transfected Neuro-2a cells at 5 hours after 0.5 μM STS treatment. The quantitative analysis is shown in (E) (F) and (I). (G-H) PTBP1 knockdown reduces early apoptotic cells at 5 hours after 0.5 μM STS treatment and the apoptotic profile of flow cytometry is shown in (G). Data are represented as the mean ± SD of four independent replicates. N=4; ***, $p<0.001$; two-tailed Student's t-test compared with siCtr-transfected cells.
(I) Quantification of cleaved caspase 3 protein levels from Western blot analysis in (D).
(J) Diagram of the *Bak1* exon 5 minigenes. The backbone structure is in grey and the inserted *Bak1* exon 5 and flanking introns are in yellow. The mutated bases in Mut construct are in red.
(K) PSI of WT (WT) and mutant (Mut) *Bak1-E5* minigene in Ctr- and shPTBP1-transfected Neuro-2a cells. Data are represented as the mean ± SEM; $N_{WT}=3$, $N_{Mut}=4$; ****, $p<0.0001$; n.s., not significant; two-tailed Student's t-test compared to Ctr-transfected cells for each minigene construct. See also Figure S8 and Table S5.

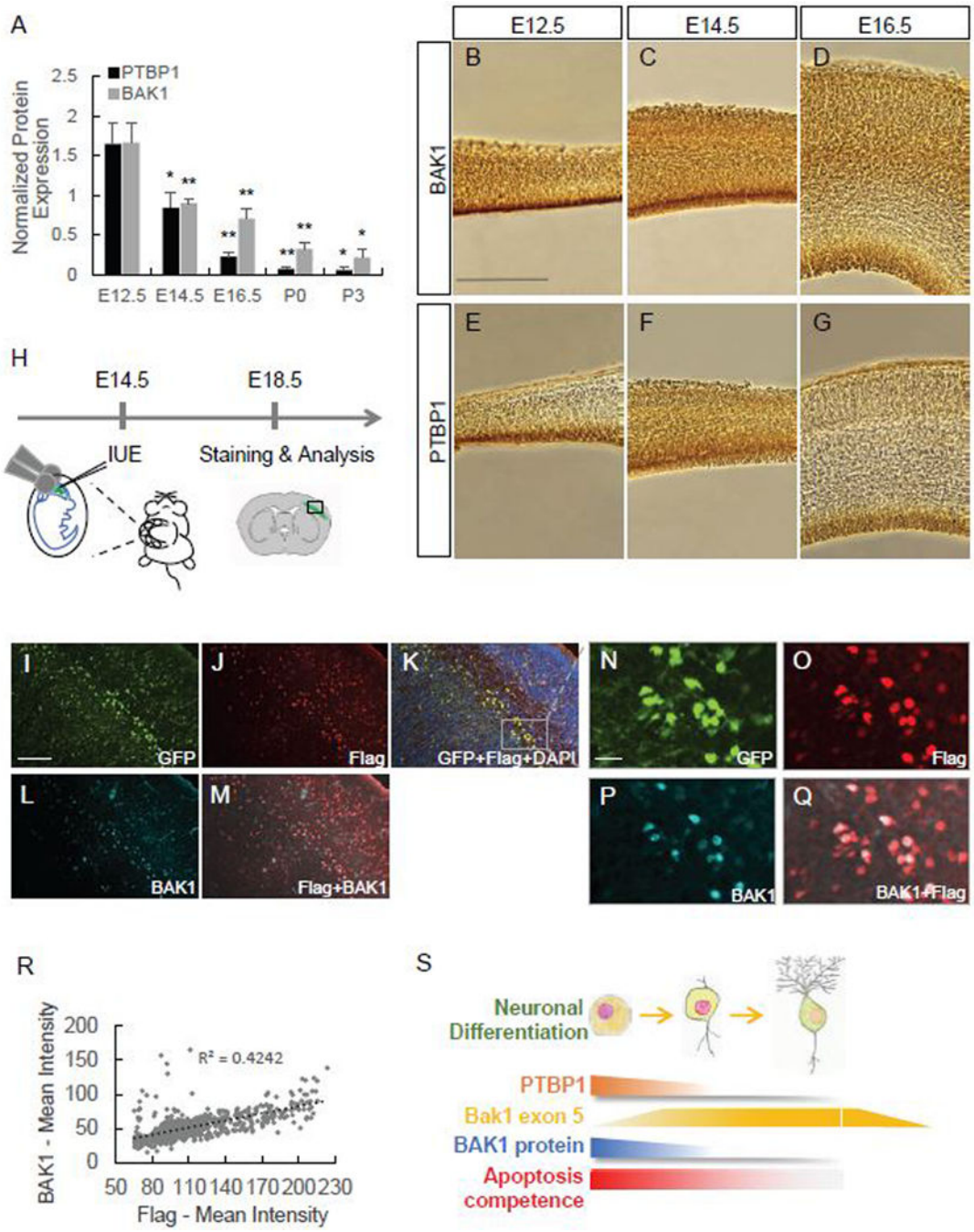


**Figure 7. Developmental PTBP1 loss is necessary for inhibiting BAK1 proteins in the mouse brain**

(A) The quantitative analysis of PTBP1 and BAK1 protein expression in WT neocortices from E12.5 to P3. The relative expression is normalized to one E14.5 cortex in each Western blot. Data are represented as the mean ± SEM; N=3–9; *, $p<0.05$; **, $p<0.01$; two-tailed Student's t-test compared to the E12.5.

(B-G) Immunohistochemistry staining of BAK1 (B-D) and PTBP1 (E-G) in the WT cortices from E12.5 to E16.5. Scale bar: 250 μm.

(H) Schematic of IUE strategy for the experiments in (I-R).

(I-Q) Representative immunofluorescent images of E18.5 cortices after IUE of FLAG-PTBP1-IRES-EGFP expression plasmid at E14.5. Scale bars: 100 μm in (I) and 20 μm in (N).

(R) Induced BAK1 expression is correlated with the ectopically-expressed FLAG-PTBP1. Each dot represents a $GFP^+$ cell plotting the mean intensities of BAK1 vs FLAG-PTBP1. N=683.

(S) Schematic diagram for programming apoptosis sensitivity during neuronal differentiation by PTBP1-mediated *Bak1* splicing and protein expression. See also Figures S9, S10, and S11.